

LA-UR-12-23988

Approved for public release; distribution is unlimited.

Title: Magneto-inertial fusion FRCHX Experiments at AFRL

Author(s): Wurden, Glen A.; Intrator, Thomas P.; Weber, Thomas; Degnan, J. H.; Amdahl, D. J.; Domonkos, M. T.; Grabowski, T. C.; Ruden, E. L.; White, W. M.; Frese, M. H.; Frese, S. D.; Camacho, J. F.; Coffey, Sean K.; Roderick, N. F.; Kostora, M. R.; Sommars, W.; Kiutu, G. F.; Bauer, B. S.; Fuelling, S. F.; Yates, K.; Lynn, A. G.

Intended for: CT2012: Advanced Controls and Diagnostics for Confinement  
Improvements of Compact Toroids, 2012-09-25/2012-09-28 (Newport Beach, California, United States)



Disclaimer:

Los Alamos National Laboratory, an affirmative action/equal opportunity employer, is operated by the Los Alamos National Security, LLC for the National Nuclear Security Administration of the U.S. Department of Energy under contract DE-AC52-06NA25396. By approving this article, the publisher recognizes that the U.S. Government retains nonexclusive, royalty-free license to publish or reproduce the published form of this contribution, or to allow others to do so, for U.S. Government purposes.

Los Alamos National Laboratory requests that the publisher identify this article as work performed under the auspices of the U.S. Department of Energy. Los Alamos National Laboratory strongly supports academic freedom and a researcher's right to publish; as an institution, however, the Laboratory does not endorse the viewpoint of a publication or guarantee its technical correctness.

# **Magneto-inertial fusion FRCHX experiments at AFRL**

---

US-Japan CT Workshop 2012

Sept. 25, 2012

Glen A. Wurden

G. A. Wurden, T. Weber, T. Intrator

*Los Alamos National Laboratory, MS-E526, Los Alamos, New Mexico, USA 87545*

*J. H. Degnan, D. J. Amdahl, M. Domonkos, C. Grabowski, E. L. Ruden, W. M. White*

*Air Force Research Laboratory, Kirtland Air Force Base, New Mexico, USA 87117*

*M. H. Frese, S. D. Frese, J. F. Camacho, S. K. Coffey, N. F. Roderick*

*NumerEx, LLC, Albuquerque, New Mexico, USA 87106*

*M. Kostora, W. Sommars, SAIC, Albuquerque, New Mexico USA 81313*

*G. F. Kiutu, VariTech Services, Albuquerque, NM 87112*

*B. Bauer, S. R. Fuelling, K. Yates, University of Nevada, Reno, Nevada, USA 89557*

*A. G. Lynn, University of New Mexico, Albuquerque, NM 87131*

Magneto-Inertial Fusion (MIF) approaches take advantage of embedded magnetic field to improve plasma energy confinement by reducing thermal conduction relative to conventional inertial confinement fusion (ICF). MIF reduces required precision in the implosion and the convergence ratio. Since 2008, AFRL and LANL have developed one version of MIF. We have (1) reliably formed, translated, and captured Field Reversed Configurations (FRCs) in magnetic mirrors inside metal shells or liners in preparation for subsequent compression by liner implosion; (2) imploded a liner with interior magnetic mirror field, obtaining evidence for compression of 1.36 T field to 540 T; (3) performed a full system experiment of FRC formation, translation, capture, and imploding liner compression operation; (4) identified by comparison of 2D-MHD simulation and experiments factors limiting the closed- field lifetime of FRCs to about half that required for good liner compression of FRCs to multi-keV,  $10^{19}$  ion/cm $^3$ , high energy density plasma (HEDP) conditions; and (5) designed and prepared hardware to increase that closed field FRC lifetime to the required amount. We have just won a 1-year extension of our magneto-inertial fusion experiment with liner compression of FRC plasmas in the FRCHX experiment at Shiva Star. We will summarize the present status of the experiment, and our plans for the upcoming year. Various experimental approaches to extending the lifetime of the target FRC plasma, through higher flux formation, better trapping, and instability suppression will be described. Hardware for this purpose includes two kinds of RF preionization, gas-puff prefill, biased potential rings for rotation suppression, modification of the magnetic profile in the trapping region (including a longer trap and larger mirror), modeling of elimination of the translation section, and studying plasma guns for aided FRC formation in FRX-L at LANL. New diagnostics are also being added to FRCHX, including multi-frame end-on soft x-ray imaging, side-view schlieren imaging, and multi-chord snapshot visible spectroscopy. This work is supported by the Fusion Energy Sciences office in DOE, LANS contract DE-AC52-06NA25396, & AFRL Interagency Agreement DE-AI02-04ER54764.



---



# Magneto-Inertial Fusion (Magnetized Target Fusion)

---

- A hybrid approach (magnetic + inertial) to achieving fusion plasmas in the laboratory
- It allows access to 1-1000 Megabar pressures and multi-Megagauss fields with macro-scale plasmas
- Magnetic fields allow the use of lower velocity drivers for Inertial Fusion Energy (IFE), lower convergence ratios, and larger tamping; which we believe are key advantages
- Experiments with significant neutron yields are possible in the near term
- I will focus on the LANL/AFRL collaboration, with FRCHX (Field Reversed Compression and Heating Experiment), operational at the Air Force Research Laboratory (AFRL) in Albuquerque since 2008 as an FRC source.



---



# This is not a new idea: Previous liner implosion solutions

## The Fast Liner Reactor

A.R. Sherwood, B.L. Freeman, R.A. Gerwin, T.R. Jarboe,  
R.A. Krakowski, R.C. Malone, J. Marshall, R.L. Miller, B.  
Suydam

Los Alamos Scientific Laboratory, LA-6707-P, (1977)

## Title: Fast liner proposal

**Abstract:** This is a proposal to study, both theoretically and experimentally, the possibility of making a fusion reactor by magnetically imploding a cylindrical metallic shell on a prepared plasma. The approach is characterized by the following features: (1) the non-rotating liner would be driven by an axial current, (2) the plasma would also carry an axial current that provides an azimuthal magnetic field for thermal insulation in both the radial and longitudinal directions, (3) solid end plugs would be utilized to prevent axial loss of particles, and (4) liner speeds would be in the  $10^6$  cm/s range. Our preliminary calculations indicate (1) that the energetics are favorable (energy inputs of about 10 MJ might produce a machine in the break-even regime), (2) that radiation and heat losses could be made tolerable, (3) that alpha-particle heating could be made very effective, and (4) that Taylor instabilities in a fast liner might be harmless because of the large viscosities at high pressures. A preliminary conceptual design of the sort of fusion reactor that might result from such an approach is discussed, as are some of the relevant reactor scaling arguments.

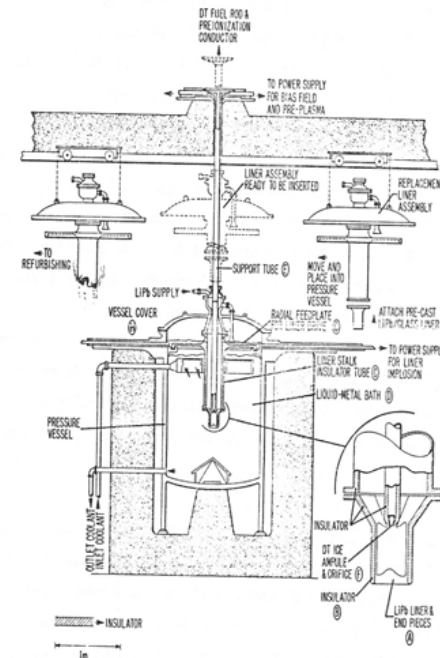
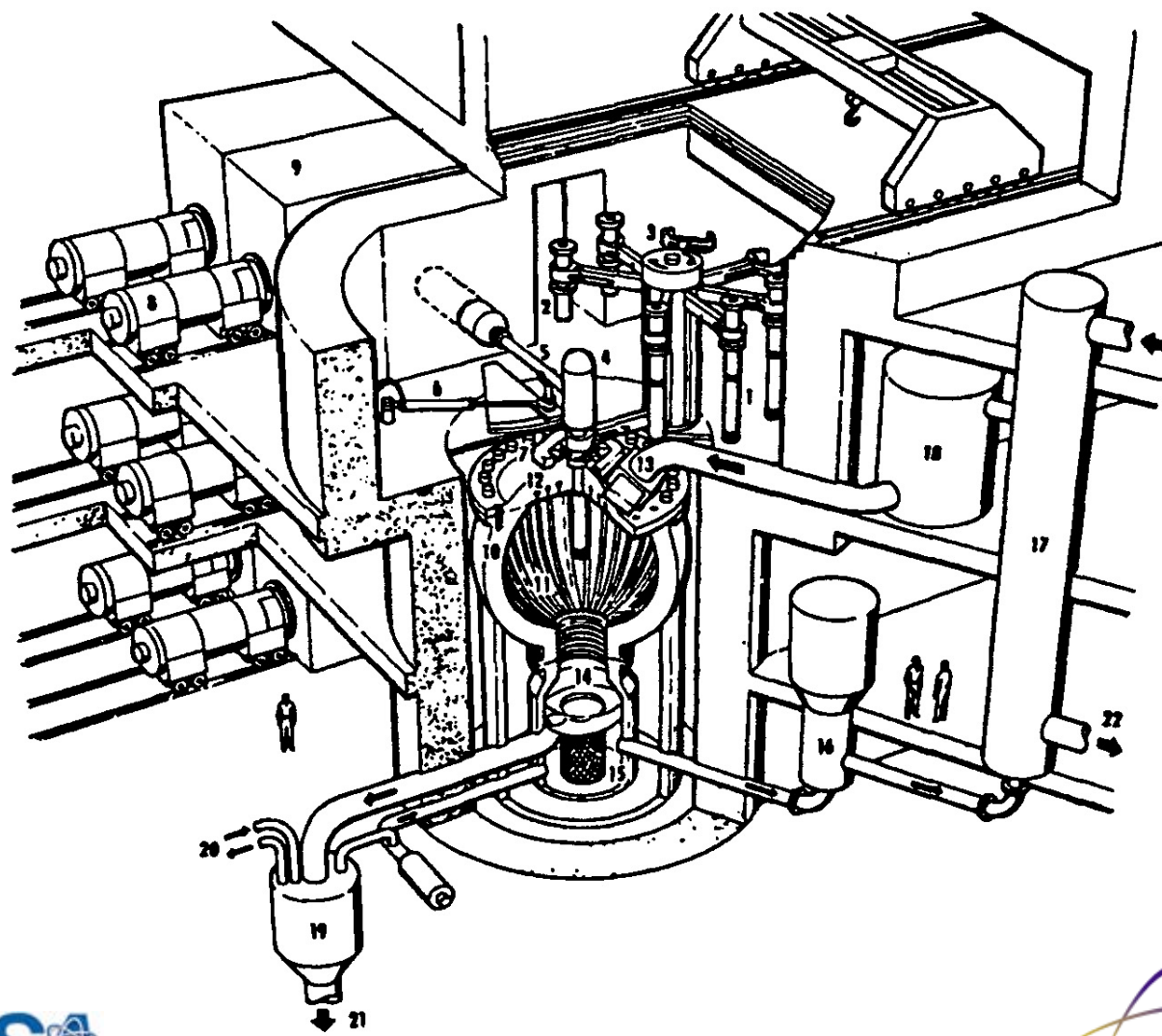


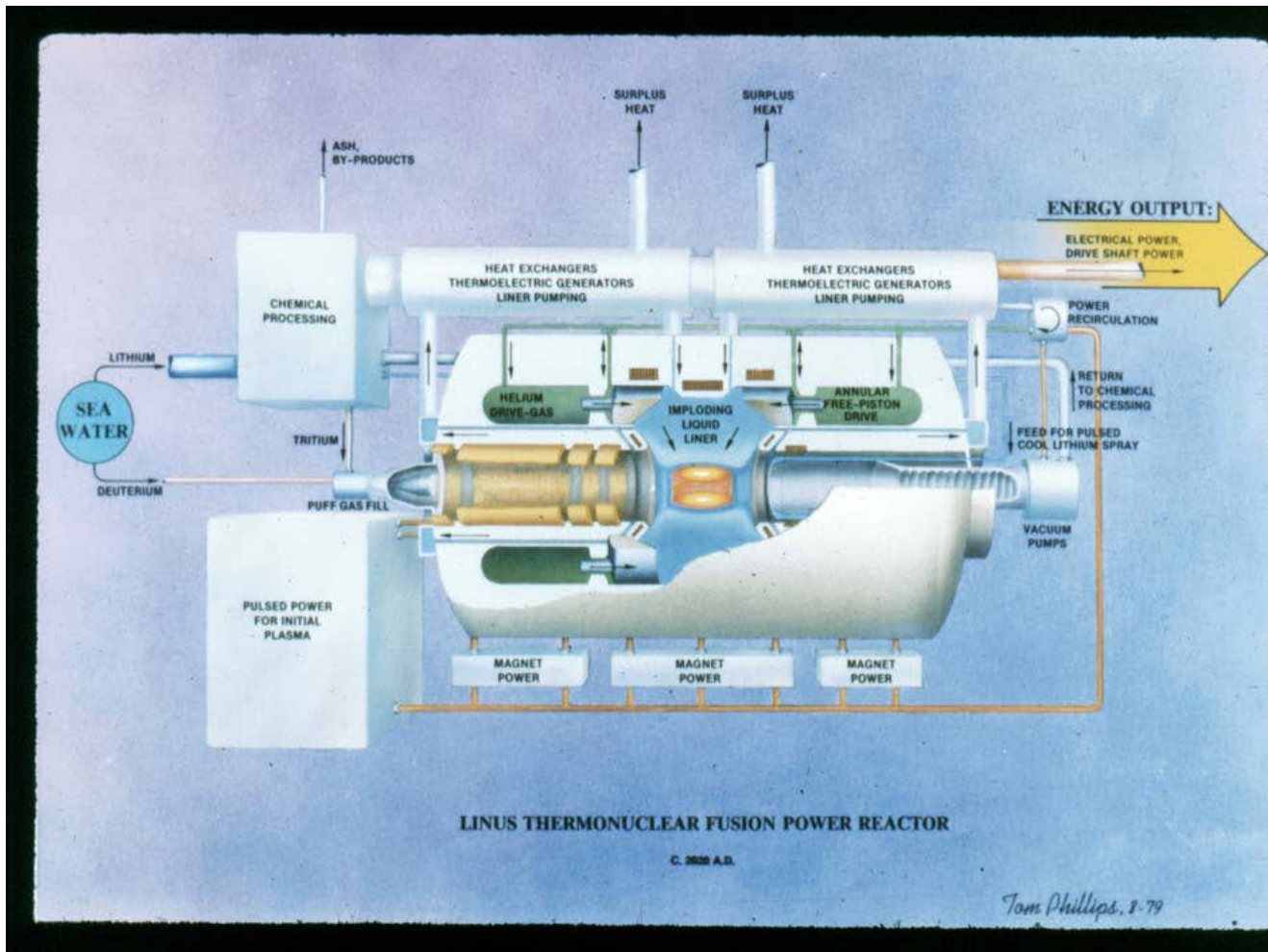
Fig. IV-6.

# LANL Fast Liner Power plant schematic (LA-7686-MS Krakowski, et al. Feb 1979)

---



# NRL's LINUS (Slow Liner) Study 1979



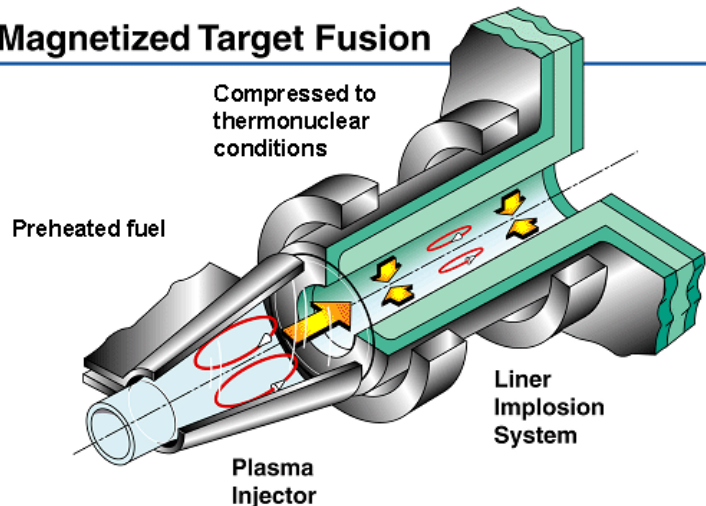
The real issue however was, what plasma (lifetime) was actually compatible with this driver?

# Magnetized Target Fusion (FRC)

CIC-1/00-0126 (11-99)



## Magnetized Target Fusion



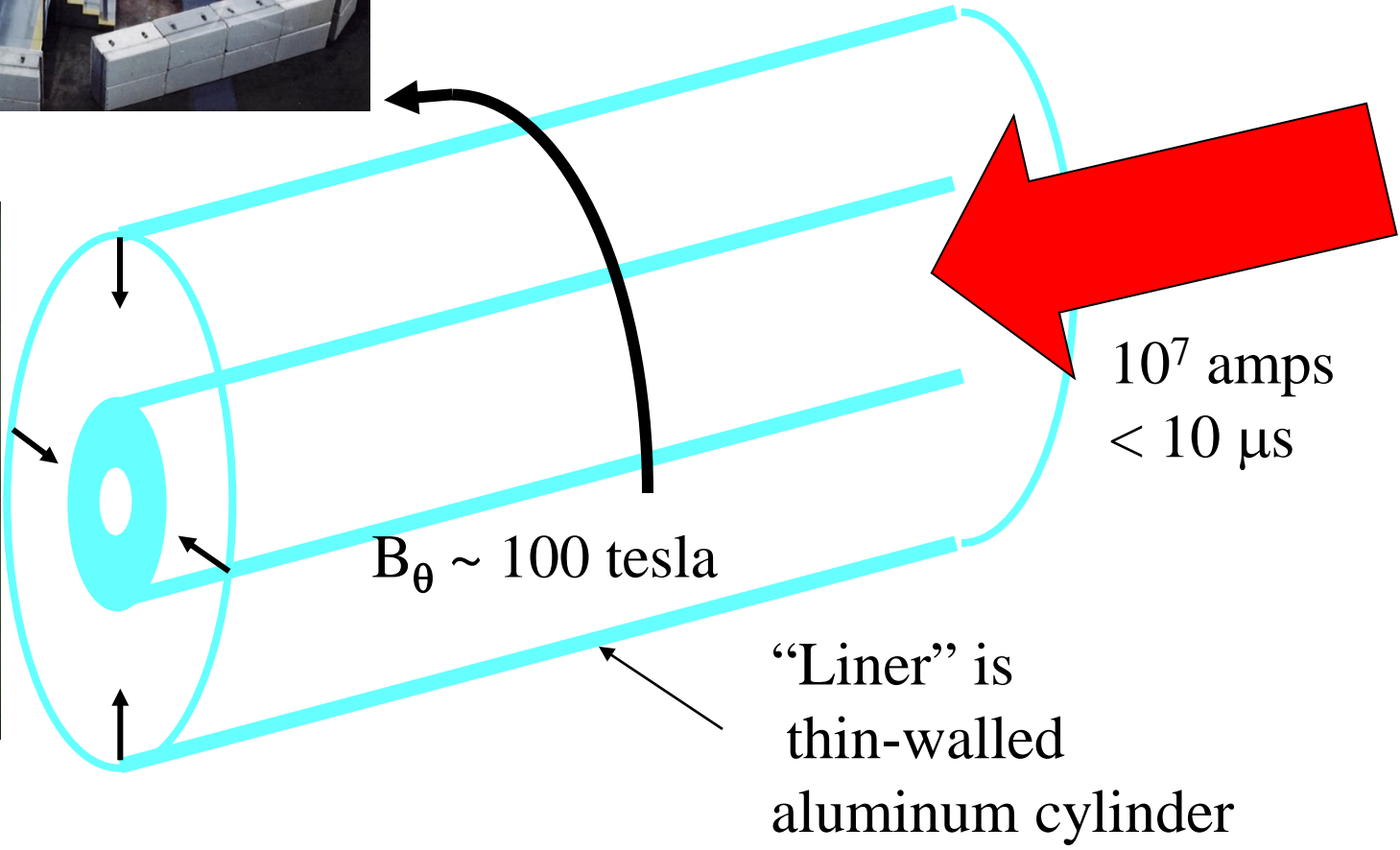
**This is a fusion concept where:**

- The plasma beta ranges from 0.8 to 1
- The heart of the device fits on a modest table-top
- The plasma density is intermediate  $\sim 10^{19} \text{ cm}^{-3}$  (MFE  $\sim 10^{14} \text{ cm}^{-3}$ , ICF  $\sim 10^{25} \text{ cm}^{-3}$ )
- The current density can be  $1000 \text{ MA/m}^2$
- The magnetic field confining the plasma is 500 Tesla !
- The auxiliary heating power level is  $\sim 1000$  Gigawatts !
- HEDP achieved by “slow” adiabatic compression (to  $\sim 1$  MBar)
- Research can be conducted with existing facilities and technologies
- In a reactor, on each pulse the liquid first wall is fresh  $\rightarrow$  no materials problem!
- The repetition rate would be  $\sim 0.1$  Hertz, so that there is time to clear the chamber from the previous event



## MTF (FRC) uses “can crusher” technology

A 1-mm thick aluminum liner is  
crushed smoothly by  $J_z \times B_\Theta$  force





# FRC Plasma Parameters: Before & After



- Pre- and Post-Compression FRC Parameters<sup>3</sup>
  - In formation region of experiment
    - $n \sim 10^{17} \text{ cm}^{-3}$
    - $T \sim 100 - 300 \text{ eV}$
    - Poloidal  $B \sim 2 - 5 \text{ T}$
  - After solid liner compression
    - $n > 10^{19} \text{ cm}^{-3}$
    - $T \rightarrow \text{several keV}$
    - Poloidal  $B \sim 200 - 500 \text{ T}$
- An initial energy confinement time  $\geq 20 \mu\text{s}$  is desired

<sup>3</sup> G.A. Wurden, et. al., “FRC Plasma Studies on the FRX-L Plasma Injector for MTF,” IAEA-CN-116/IC/P6-53, *Proc. from the 20th IAEA Fusion Energy Conference*, Vilamoura, Portugal, 2004.

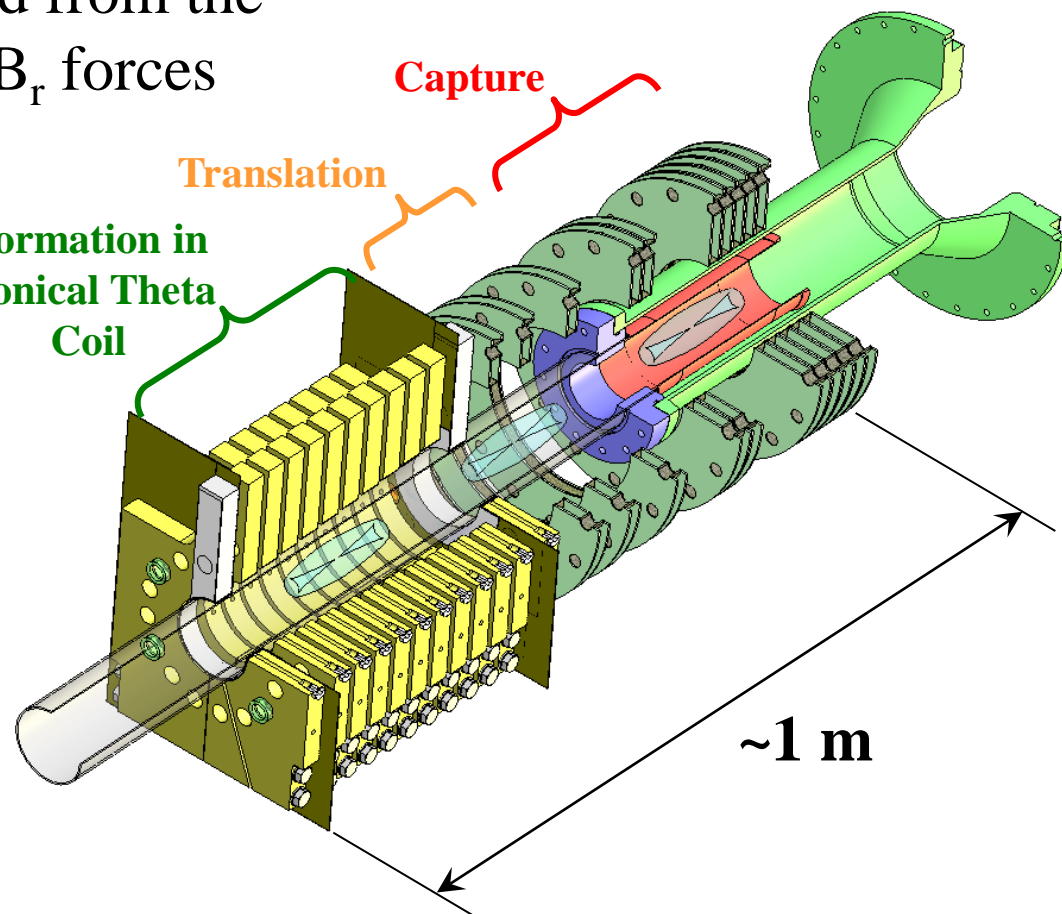


U.S. AIR FORCE

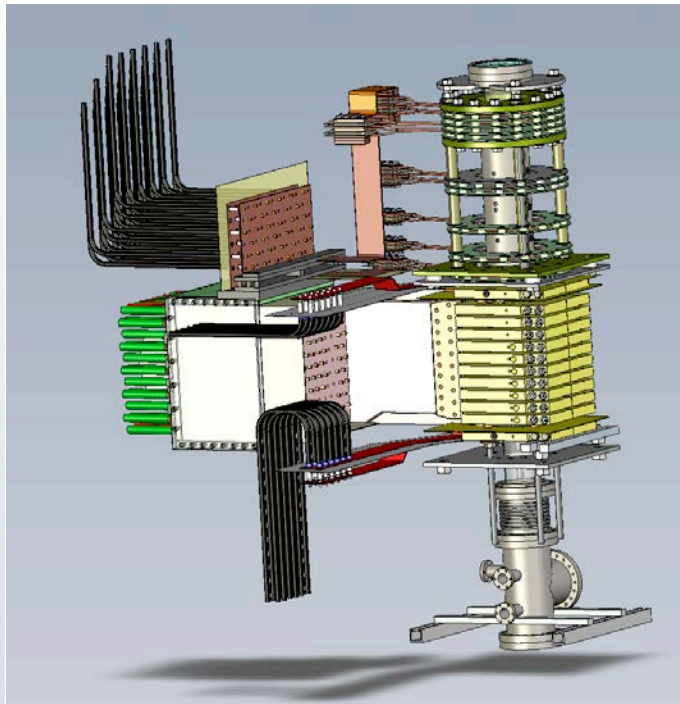
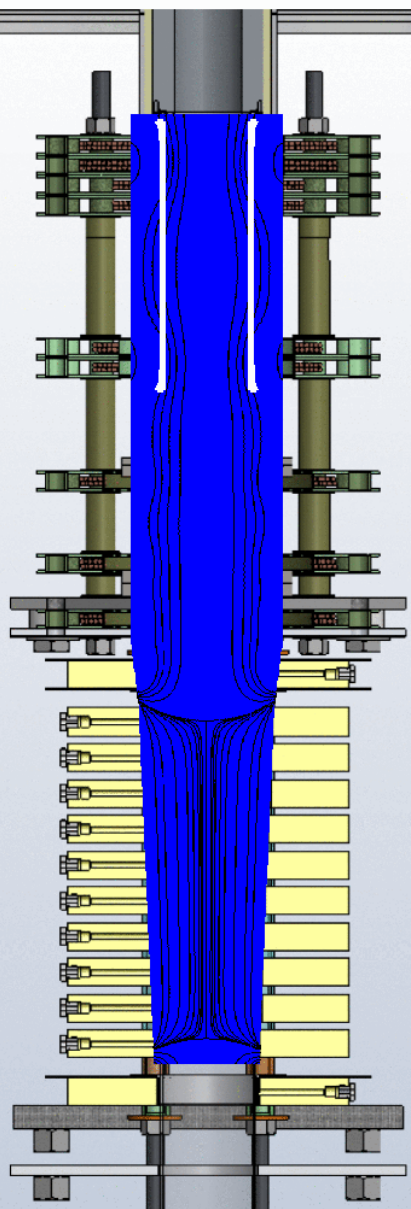
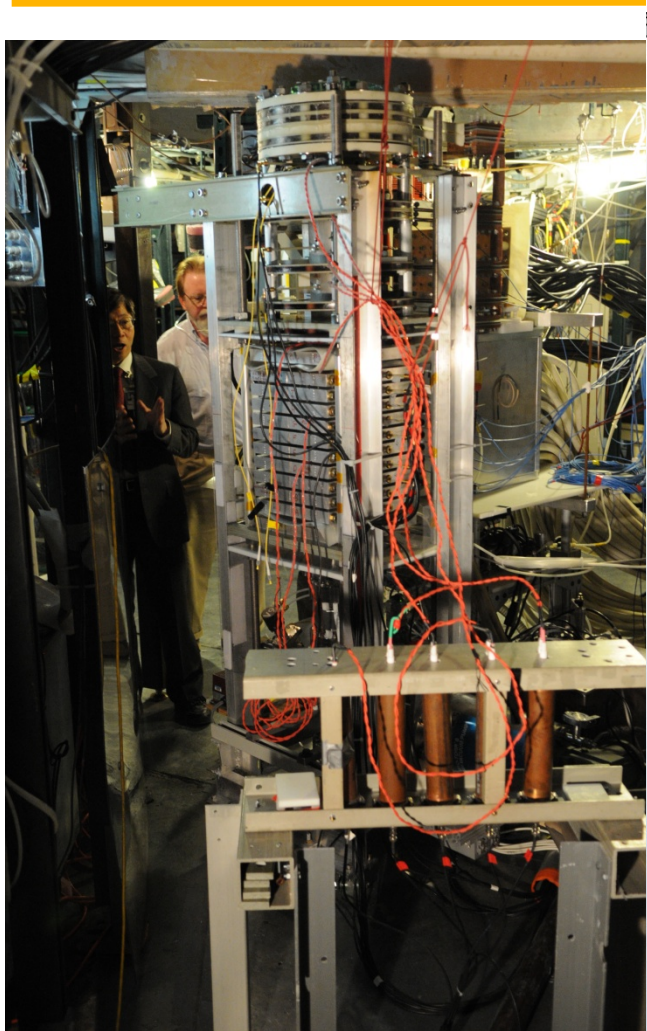
# Formation and Translation of the FRC with FRCHX



- The FRC is formed in a segmented Theta coil and then ejected from the formation region by  $J_\Theta \times B_r$  forces
- Fields along the short translation region keep the FRC from expanding
- Lower and Upper mirror fields form a capture region for the FRC that stops it within the center of the liner



# FRCHX at Shiva Star: A test of implosion physics



We have had 3 high energy engineering tests shots, followed by the first plasma/liner integrated shot in April 2010. The next shot is planned for Dec 2012, with modified timings and additional hardware to lengthen the FRC lifetime.

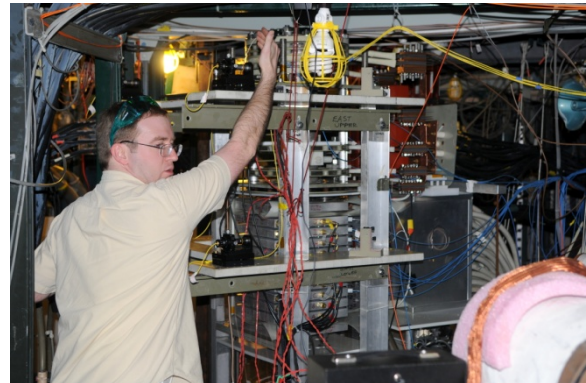
# Some of the FRCHX experiment at Shiva Star



Project leader Jim Degnan next to remains of the coils from the second engineering test shot.



Chief engineer Chris Grabowski by the FRC load stack, under Shiva Star



UNM scientist Alan Lynn adjusting multi-chord fiber interferometer on



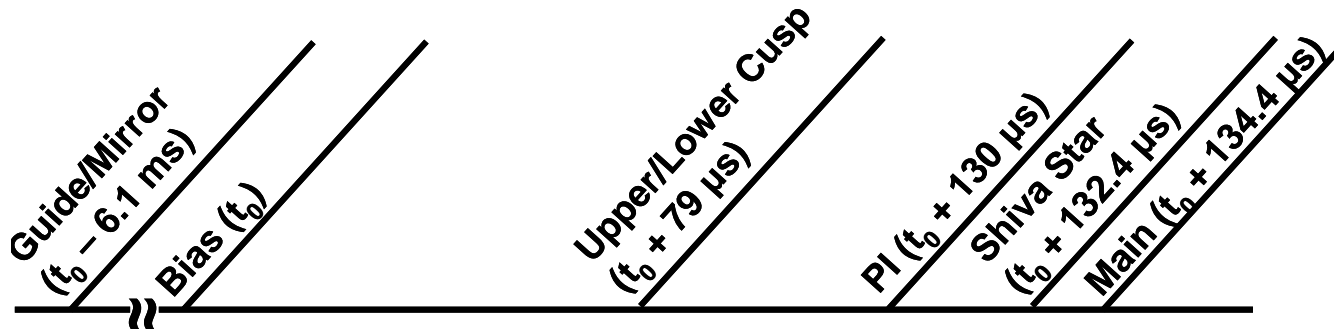
Actual deformable Aluminum liner for the next shot.  
(Slotted current return assemblies in the background)



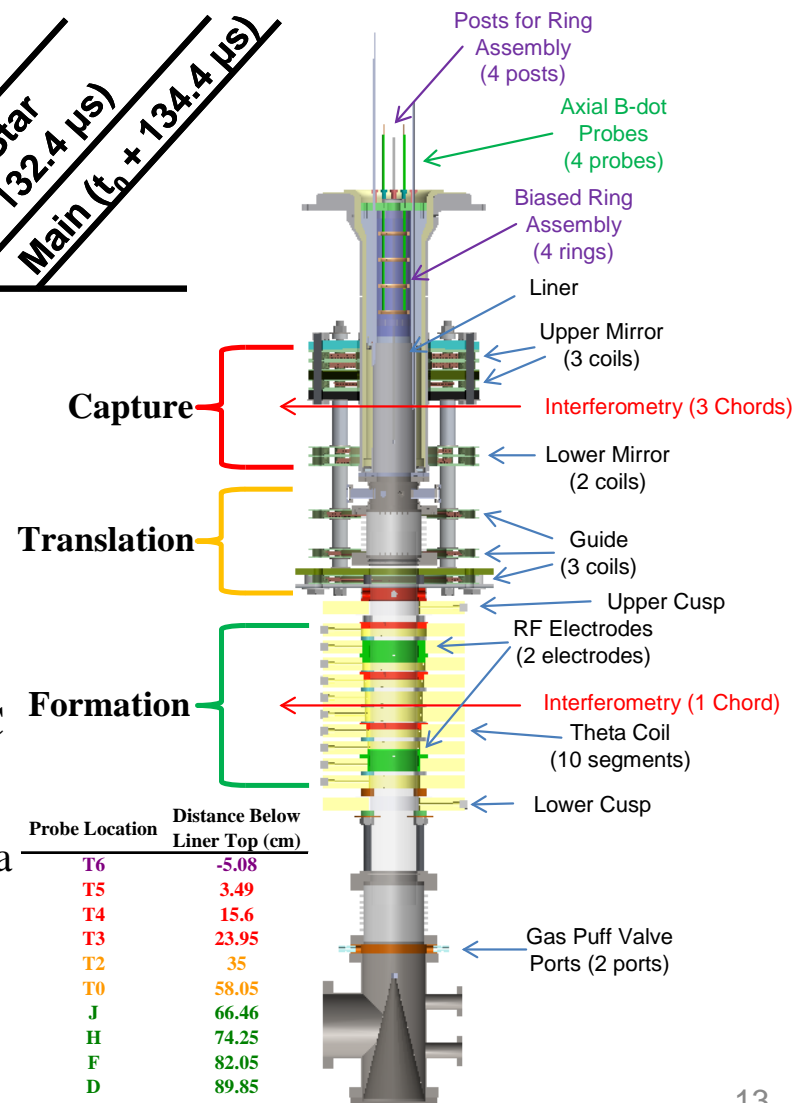
U.S. AIR FORCE



# FRCHX Field Coils and Timing



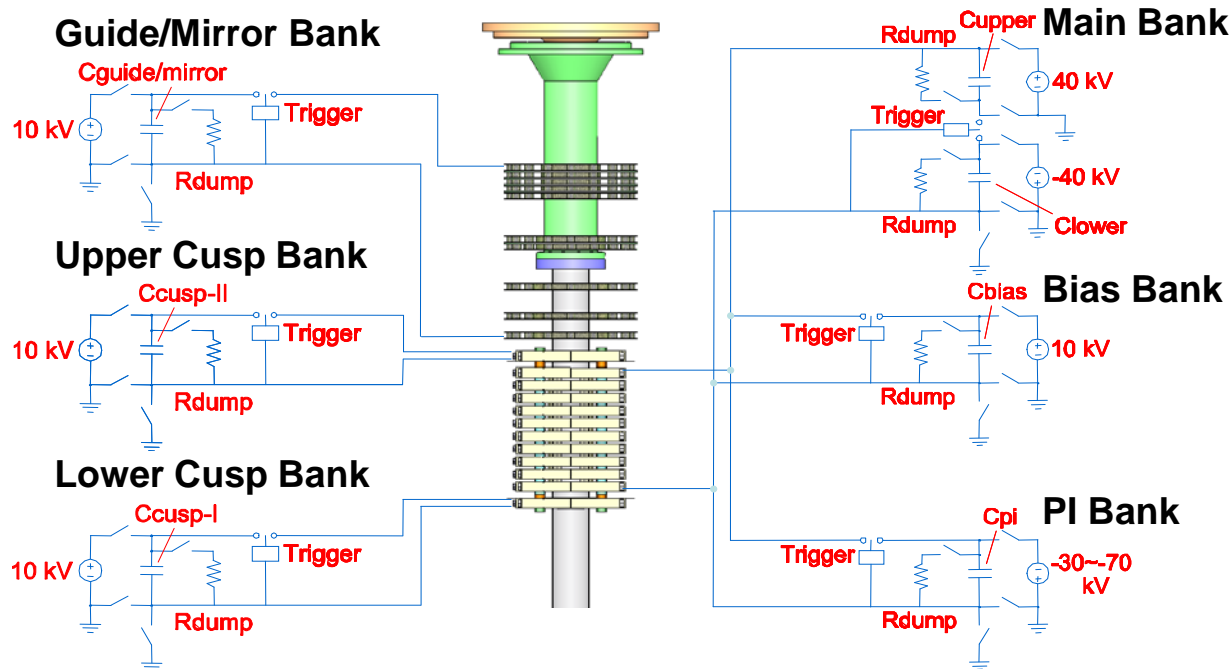
- Three discharges (from Bias, PI, & Main) drive the segmented Theta coil to form the FRC
- Guide/Mirror fields are setup first, followed by Bias field approximately 6 ms later
- Upper, Lower Cusp fields set up  $80 \sim 85 \mu\text{s}$  after Bias
- PI and Main banks triggered last to form and push the FRC up toward the liner and capture region
- $\sim 25 \mu\text{s}$  liner stagnation time requires Shiva Star discharge a few  $\mu\text{s}$  before Main discharge





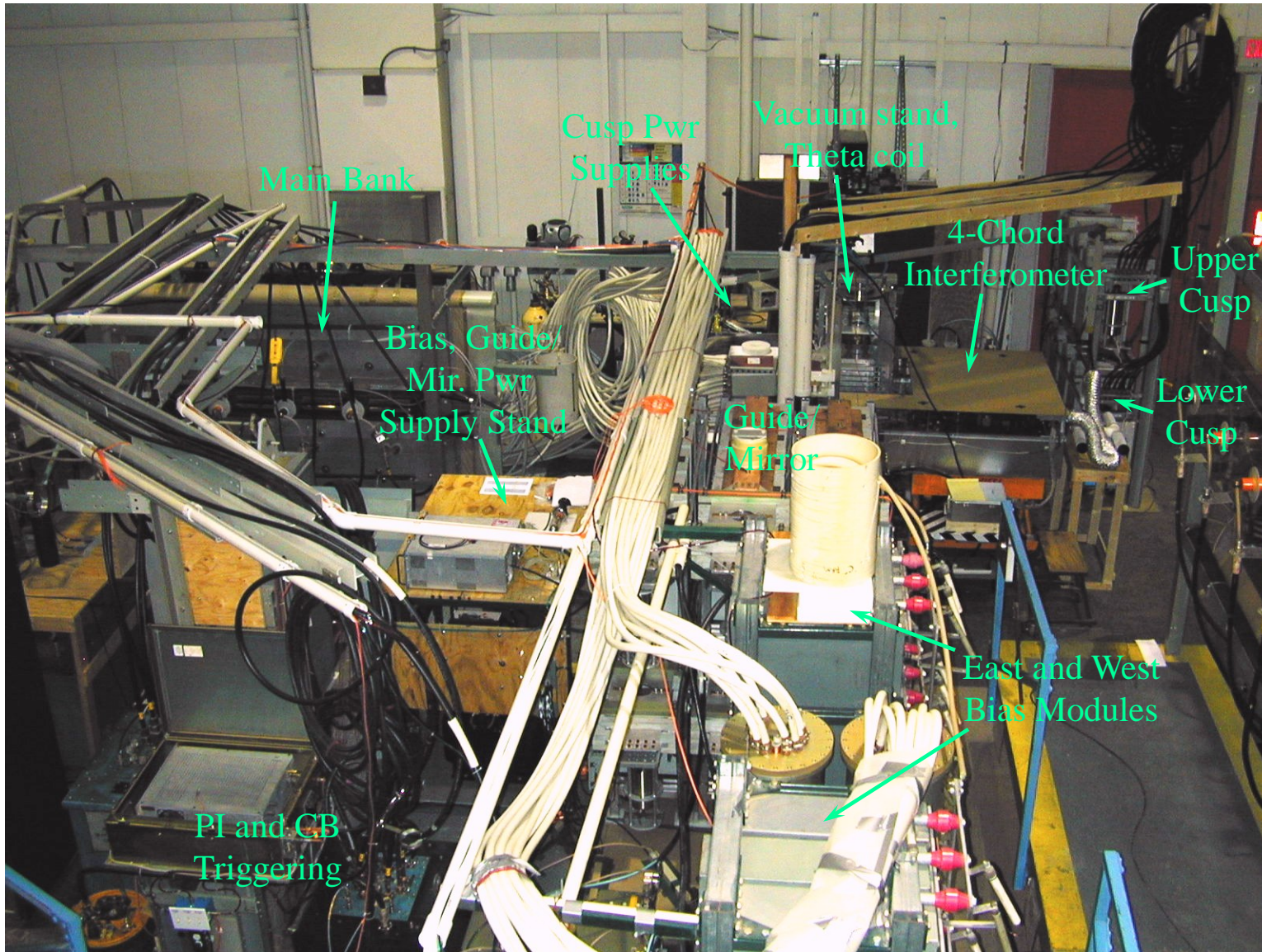
U.S. AIR FORCE

# FRCHX Pulsed Power Systems



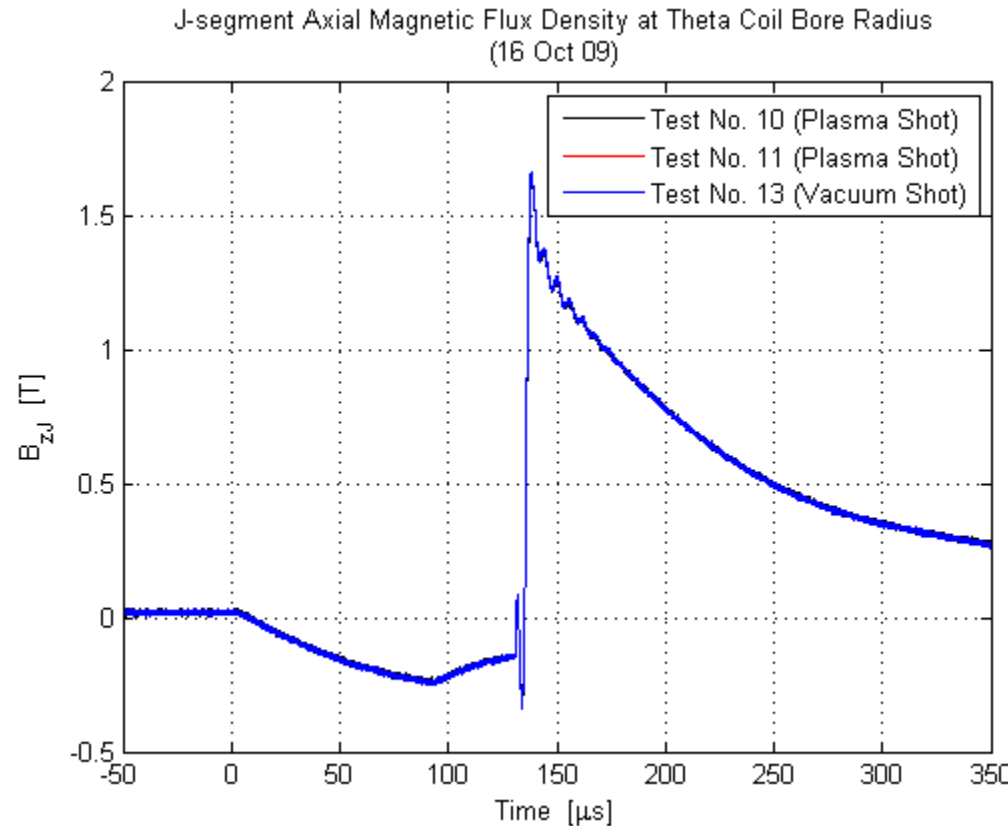
- **Bias bank** – Two capacitor bank modules,  $\sim 2.5 \text{ mF}$  per module
- **PI (Pre-Ionization) bank** – Single  $2.1 \mu\text{F}$  capacitor, oscillation frequency of  $\sim 230 \text{ kHz}$
- **Main bank** – Single *Shiva Star* bank module, caps turned sideways to reduce bank height ( $C_{upper} = C_{lower} = 72 \mu\text{F}$ ); bank is crowbarred near peak current
- **Upper and Lower Cusp banks** – Three  $500 \mu\text{F}$  capacitors each, switched with ignitrons
- **Guide/Mirror Bank** – Total capacitance of  $12 \text{ mF}$ , switched with 6 ignitrons
- **Shiva Star** – To drive the liner implosion, 36 modules,  $\sim 1.3 \text{ mF}$  total capacitance

# FRC Formation Hardware prior to moving main and PI banks under Shiva Star



## Axial magnetic probe signal shows field vs time from bias, cusp, pre-ionization, and main theta discharges

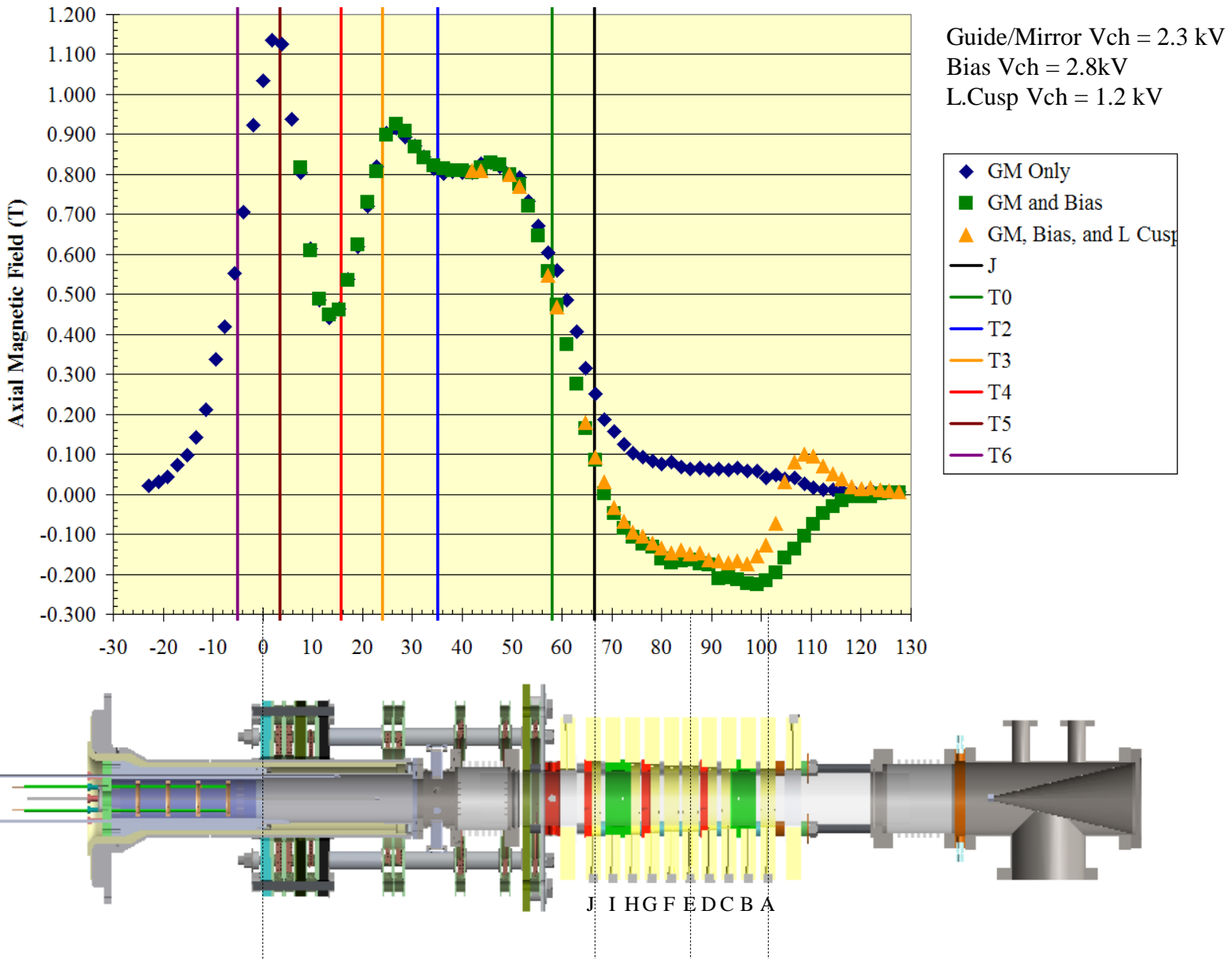
---



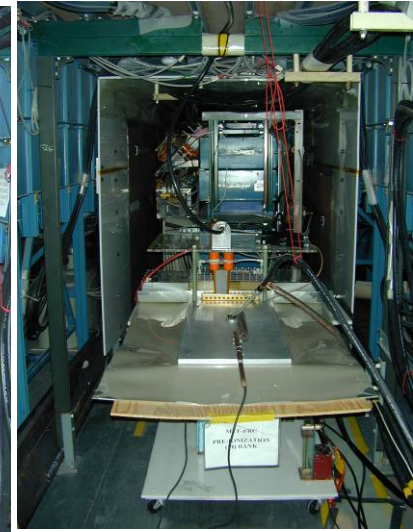
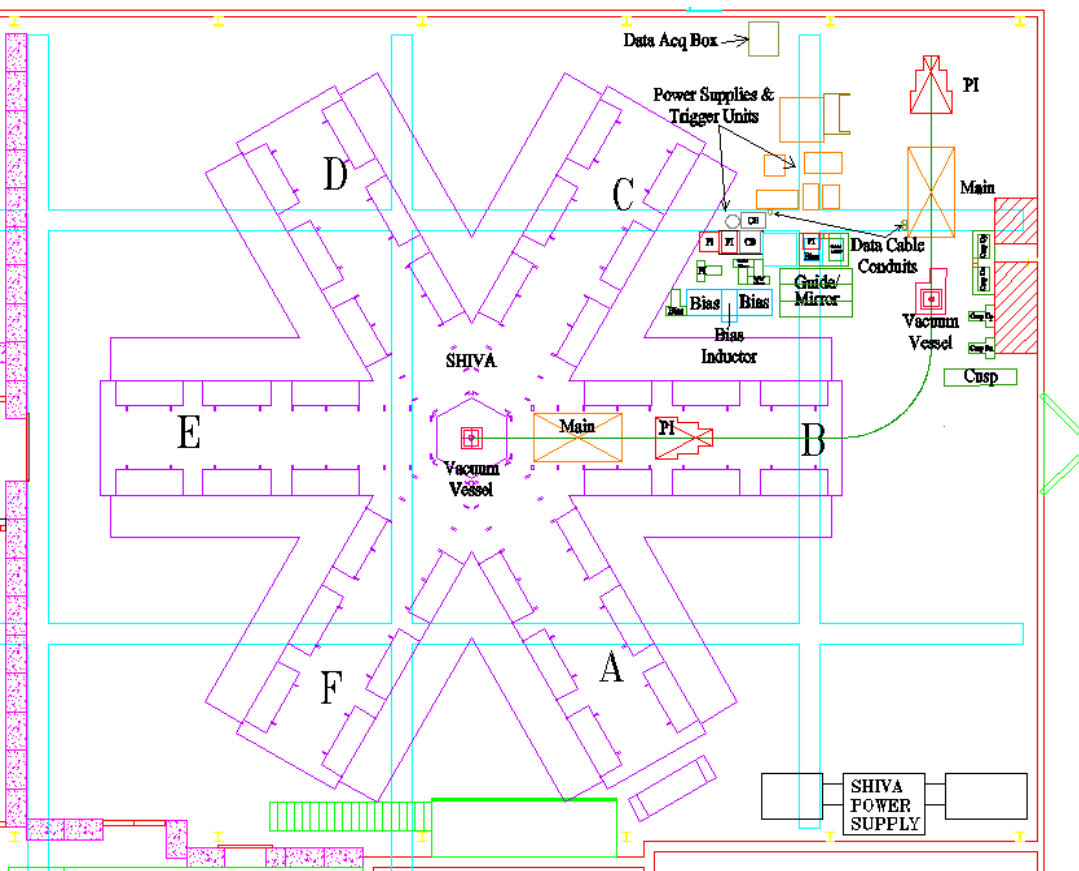
All these discharges except for the cusp discharges are through the 10 segment formation theta coil; the main theta discharge (reverse polarity with respect to the bias discharge), is crowbarred. The difference between vacuum and plasma shots is only evident at higher time resolution.

# FRCHX Axial Field Profile

(Measurements made at respective bank peaks: G/M: 6.098ms, G/M and Bias: 6.098, G/M, Bias, and L Cusp: 6.148ms)



FRCHX operates in two postions: Off to the side for setup tests, and under the center of Shiva Star for compression tests

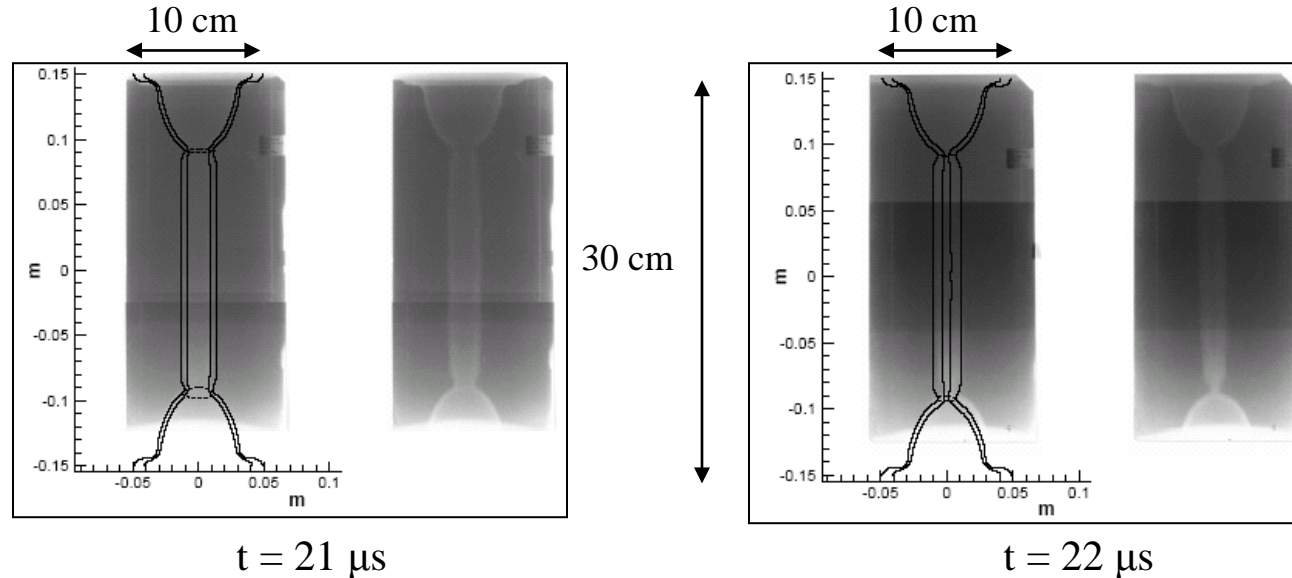


Left: illustration of locations of Shiva Star and of 6 FRC capacitor banks: guide-mirror, bias, upper and lower cusp, PI, and main theta.

Right: photos of main theta bank without and with PI bank under Shiva Star transmission line.

# Liner Implosion with void interior and 2D-MHD Simulations

Radiographs and 2D-MHD simulation results for aluminum liner implosions

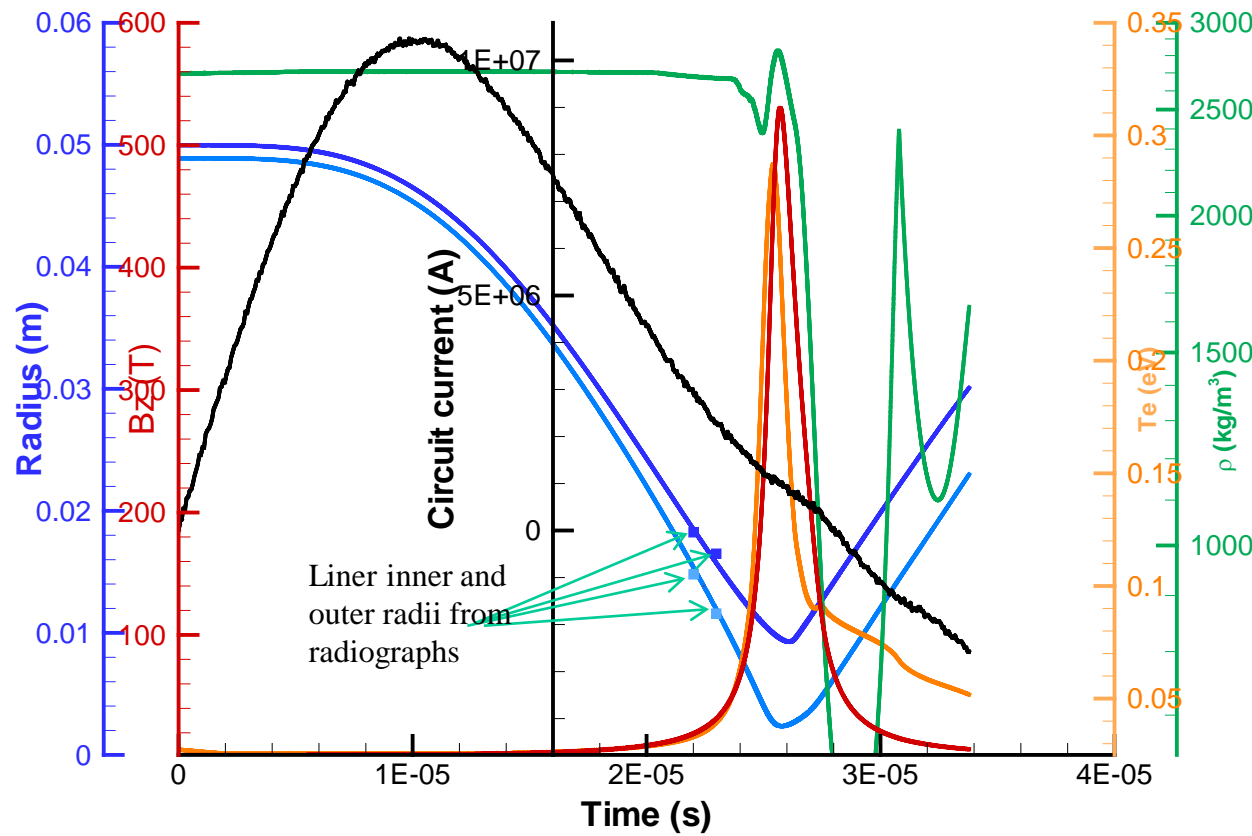


- Driven by 12 MA Shiva Star axial discharge through liner
- Shows feasibility of deformable liner / electrode contact design
- Enables 8 cm diameter electrode aperture – sufficient for FRC injection
- *Achieved 16x radial compression; 10x compression required for MTF*

*Achieved liner implosion necessary for FRC compression required for heating to multi-KeV*

# MHD simulation using experimental current agrees with radiography on liner radius vs time

MACH2 results for Shiva Star liner compression for 2 Tesla initial axial magnetic field



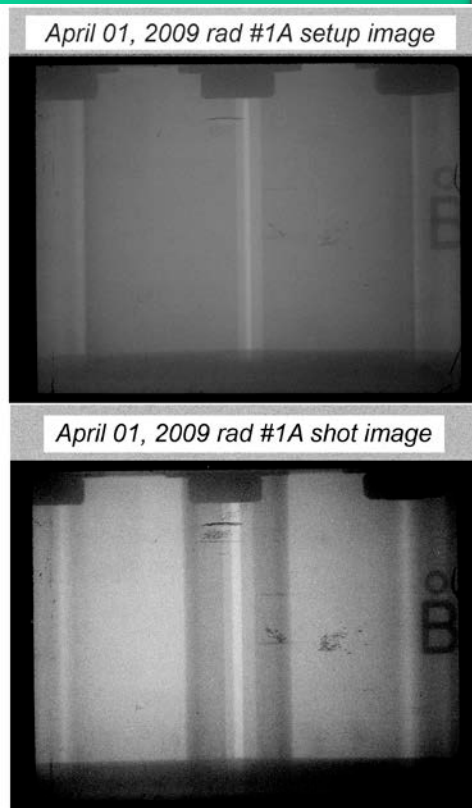
Calculated peak field is 540 Tesla

# Magnetic Field Injection and Compression Experiment

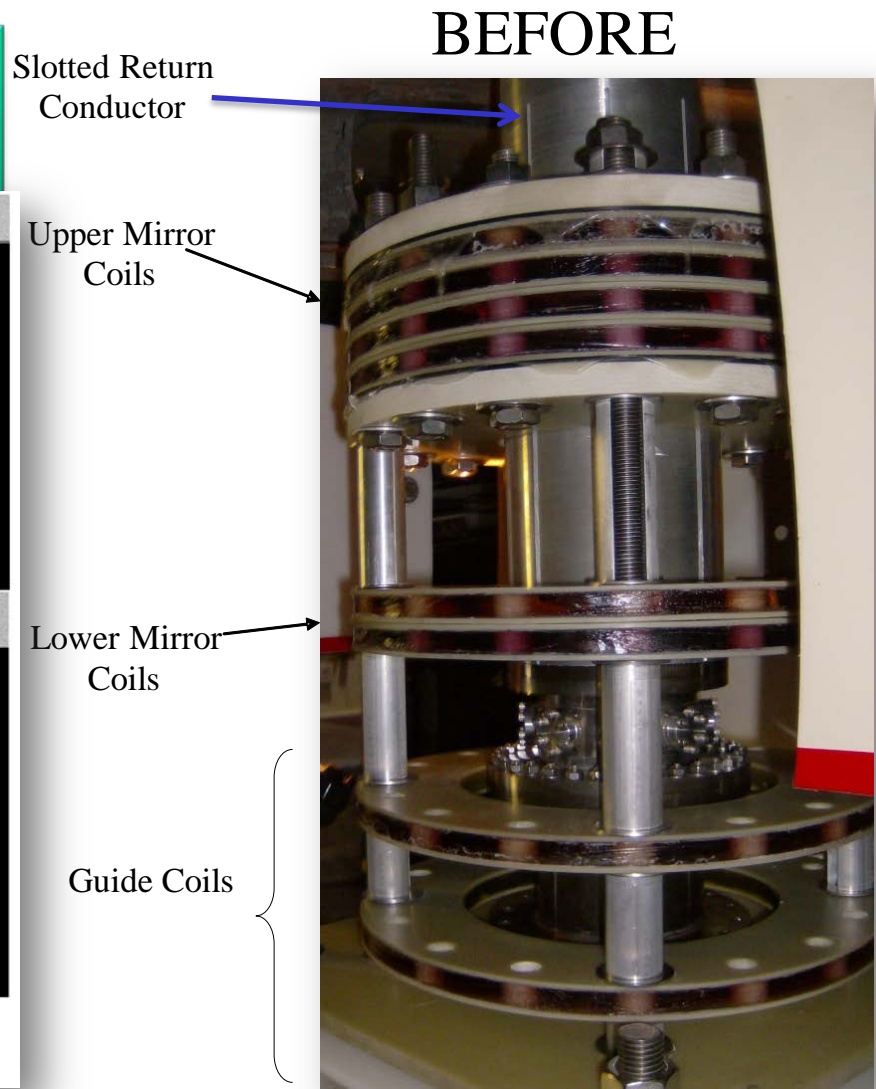
Field compression experiments have been conducted with operationally relevant field strengths.



AFTER



Note: Original liner OD = 10.0 cm  
Note2: Shot image @  $t = \sim 21.81$  usec



# Efforts at AFRL are focused on increasing the FRC lifetime (and using the lifetime that we have already demonstrated, more effectively)

---

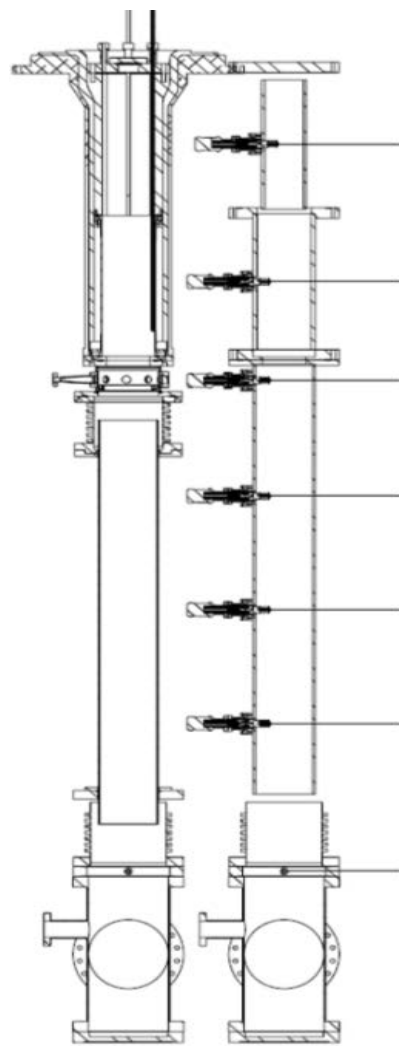
We are trying:

- Effects of low-power RF preionization
- Effects of 1-cycle high voltage “RF” boost preionization
- Control of  $n=2$  spin-up via biased rings at the upper end of FRCHX (which requires gas-puff fill hardware, in addition to our “normal” static fill)
- Raise the conventional FRC bank settings, and delay the FRC formation relative to start of liner implosion
- Changing the trapping region (longer), minimizing the translation section, and removing interfering conductors (apertures) where possible.



U.S. AIR FORCE

# Test setup for gas puff mockup, and the actual experiment

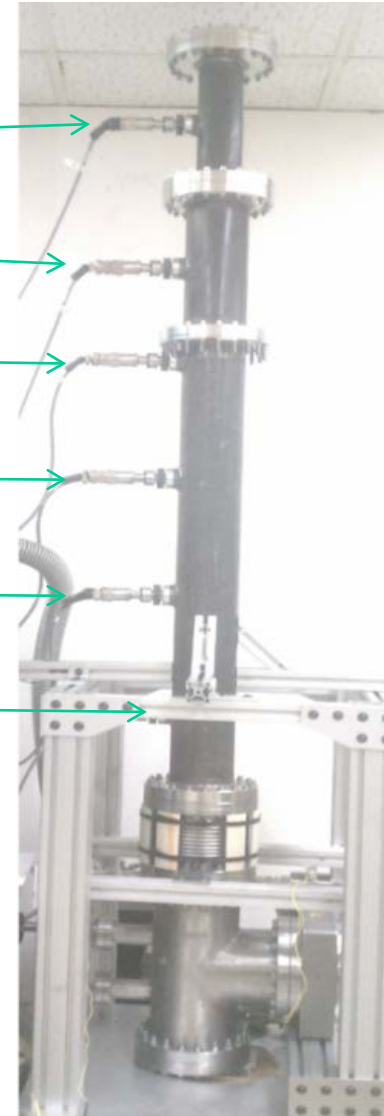


gauge position; cm  
above valve

6	155.4
5	126.0
4	104.9
3	80.2
2	55.9
1	31.6

pulsed valve position

Hidden by structure



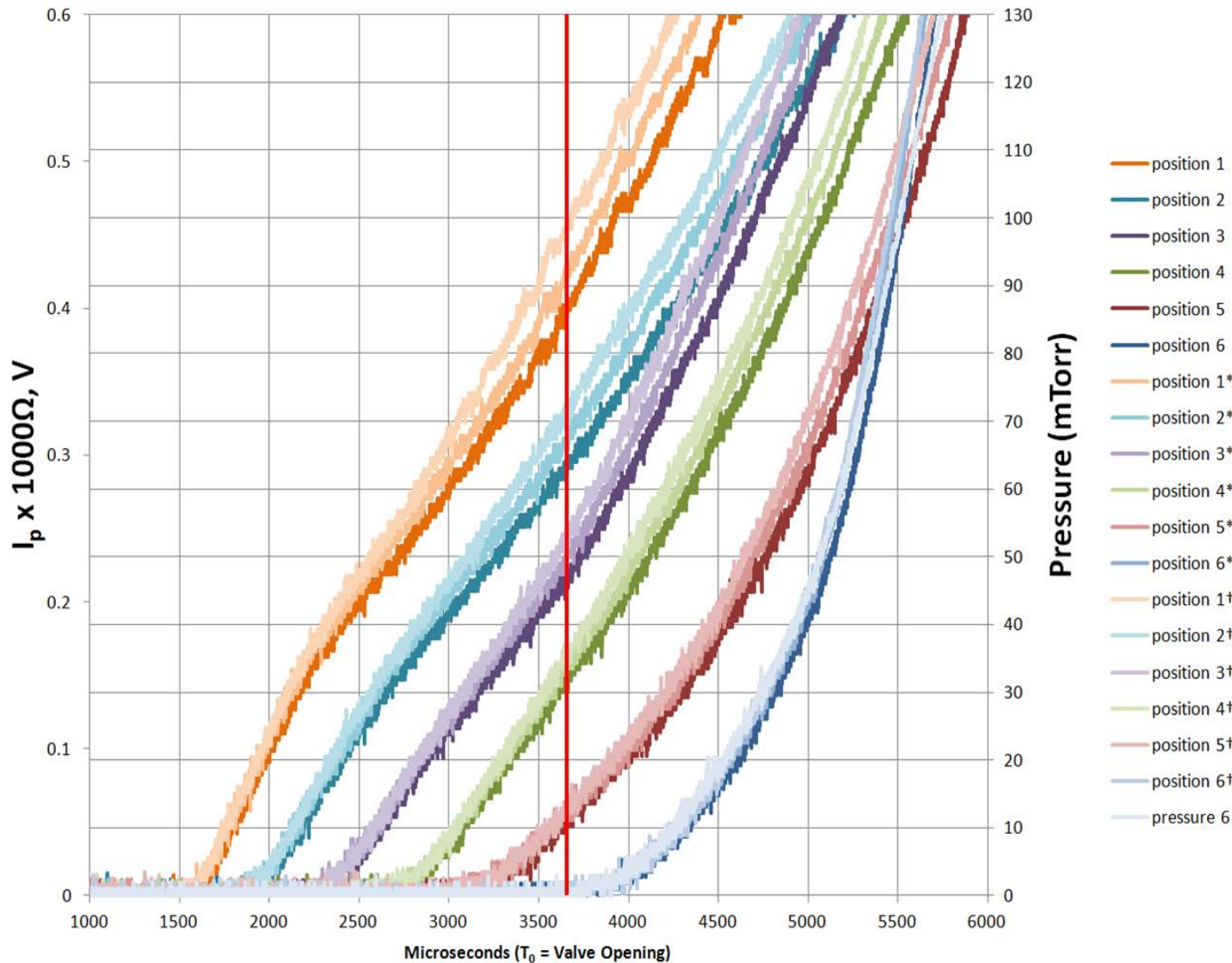


U.S. AIR FORCE

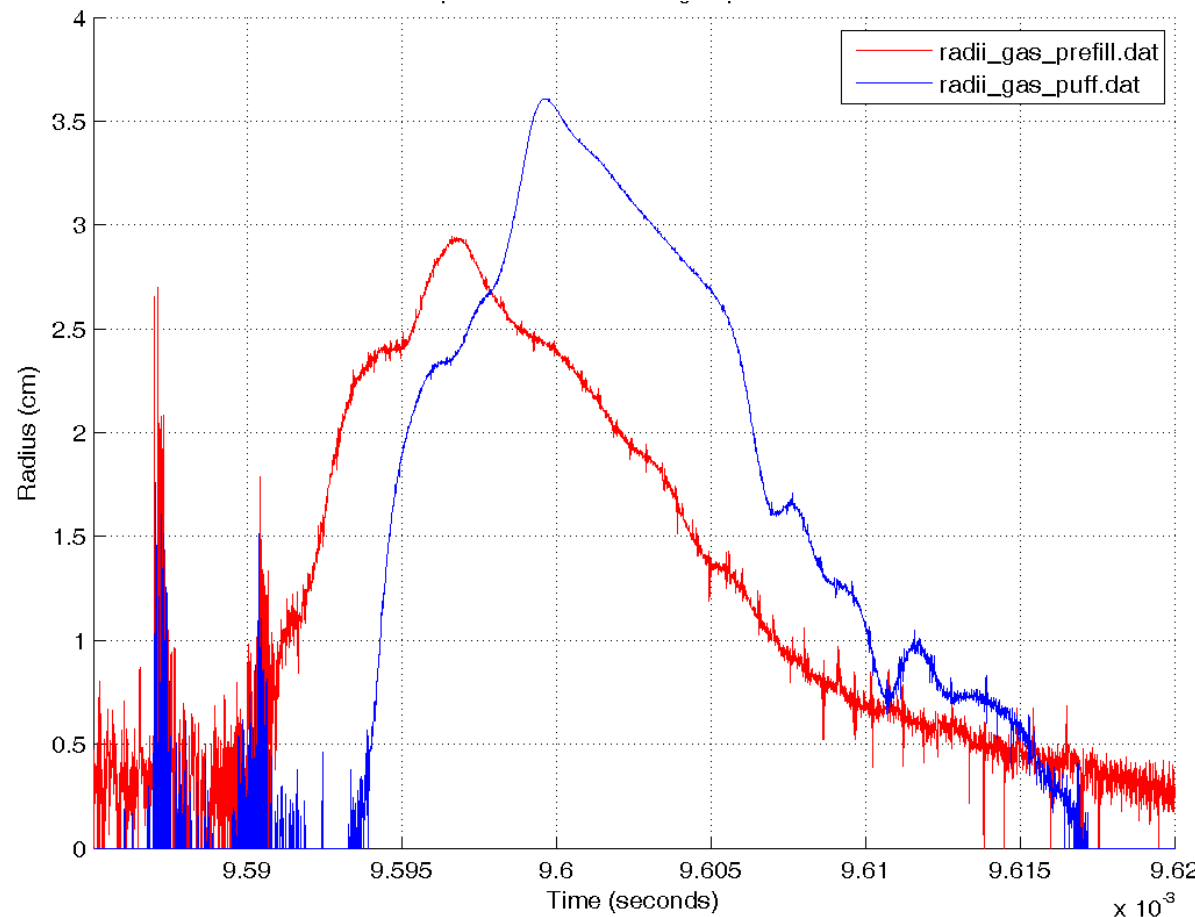
# Fast gas puffing pressure/time delay lookup table at various z-locations



6AH6 fast ion gauge signals for axial positions 1 thru 6 above valve; valve operated with 1.0 ms, 100 V. pulse, using 40 PSIA D<sub>2</sub>, 2.25 liter plenum

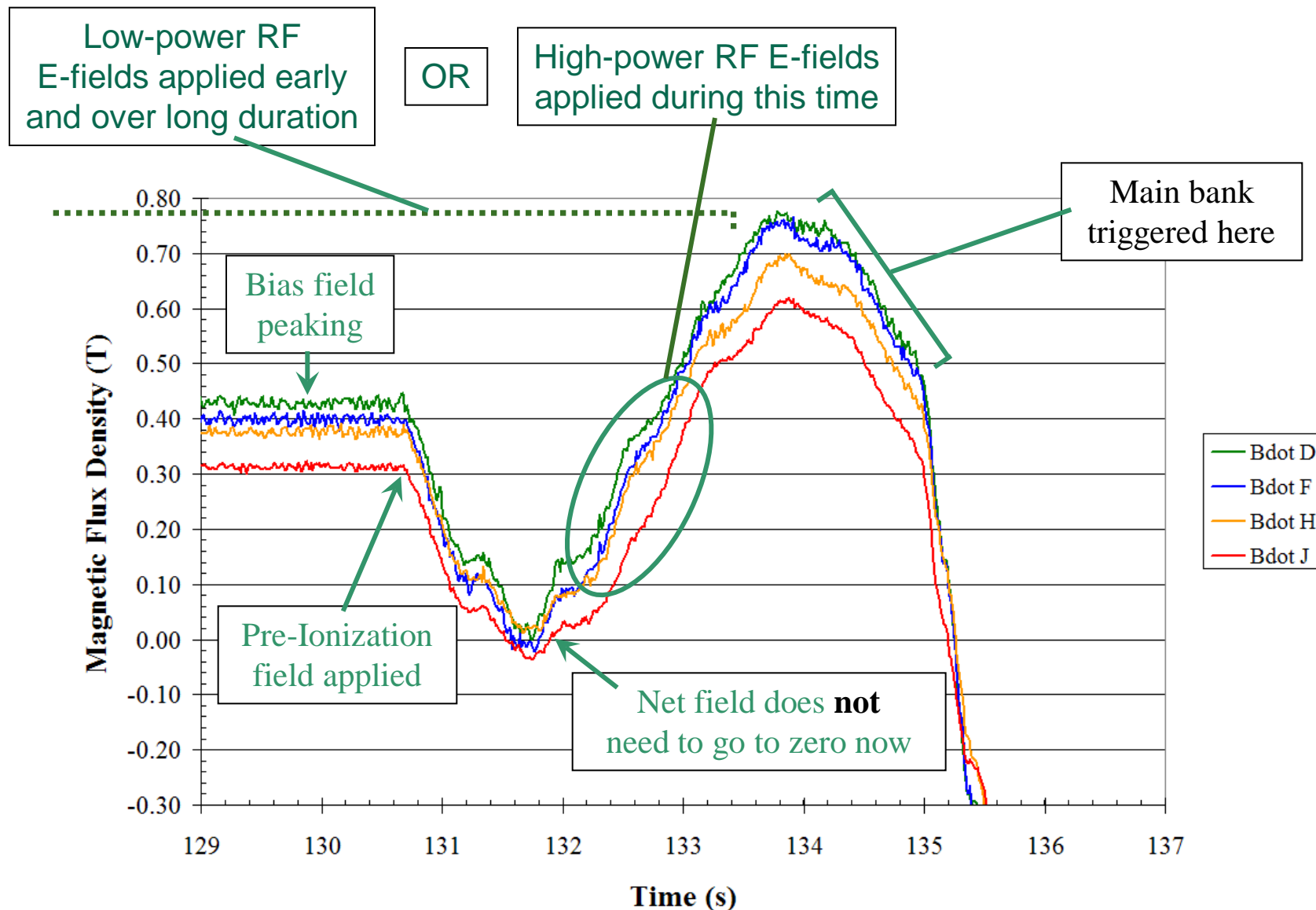


# FWHM of FRC exclusion radius vs time in the capture region is comparable for initial gas puff and optimized gas prefill FRC capture experiments



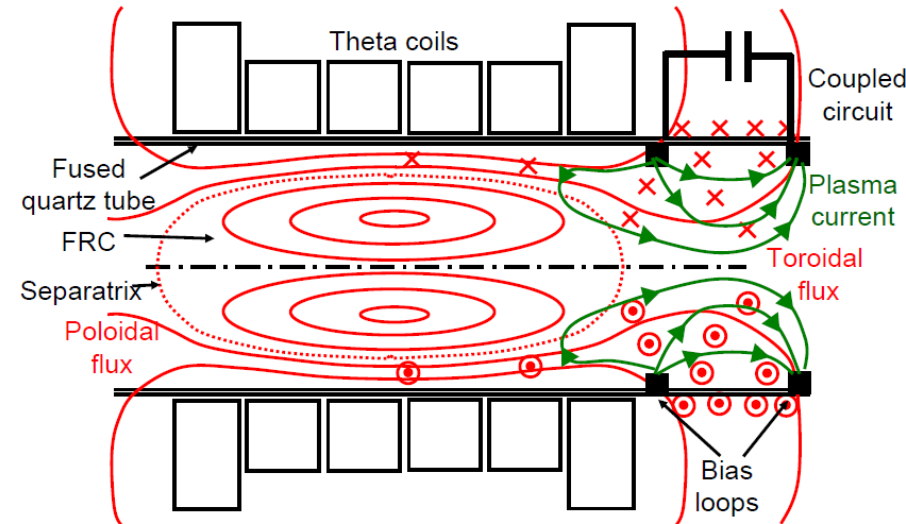
FRC exclusion radius calculated from magnetic probe signal in capture region. Its FWHM ( $\sim 12 \mu\text{s}$  in these cases) is measure of FRC lifetime. Horizontal scale is  $5 \mu\text{s}/\text{div}$ . Gas puffing enables the use of biased rings at higher voltages for attempted rotation control. 25

# Improve the FRC? Desired Scenario: Assisted breakdown via application of RF E-Fields



# Rotation Control for n=2 Stabilization

- An FRC, once formed, starts to rotate due, in part, to plasma conditions (lower temperature, higher density) at the vacuum chamber wall where the open magnetic field lines outside the separatrix exit the system.
- Generalized Ohm's Law's  $\nabla p_e$  term in the electric field implies that a non-rotating FRC will have an E field crossing the B field lines at the wall [7].
- Whether the wall is dielectric or (especially) metal, the conductivity of the wall or plasma layer there will carry current and eventually short out this E field. This current and its associated B field introduce torque at the separatrix and cause unstable viscous sheared flow across the separatrix, which leads to rotation of the FRC [8].



→ *Supporting this E field with an external circuit coupled to conducting rings placed in the B-field exit region should prevent rotation.*

<sup>7</sup> L.C. Steinhauer, "End-Shorting and," *Phys. Plasmas* **9**, pp. 3851, 2002. electric field in edge plasmas with application to field-reversed configurations

<sup>8</sup> E.L. Ruden, "The FRC's n=2 rotational instability interpreted as the dominant Rayleigh-Taylor mode of a gyroviscous plasma with sheared toroidal flow," *US-Japan exchange 2004: New directions and physics for compact toroids*, Santa Fe, NM, Sept. 14-16, 2004.

# Biased Equipotential Rings for Rotation Control

---



- Steinhauer's steady state analysis of FRC rotation due to the boundary potential of a perfectly conducting extended MHD plasma (obeying generalized Ohm's law) is used to estimate the optimal voltage in volts as being of order of the electron temperature in eV (hundred of volts).
- Steinhauer's analysis was generalized for the purpose of active field control of an FRC in Ref. [9].
- Based upon this analysis, a set of control rings has been built to implement the scheme to control rotation for most of the open flux. Gas puffing is essential to enable adequate ring voltages.
- Recently the general concept of injecting toroidal flux to introduce counter-torsional shear flow to control rotation has been implemented by T. Asai's group in Japan, and it has shown great promise [10]

<sup>9</sup> E. Ruden and M. Frese, "FRC rotation control using an electric field," 49th Annual meeting of the Division of Plasma Physics, November 12-16, 2007, Orlando, FL.

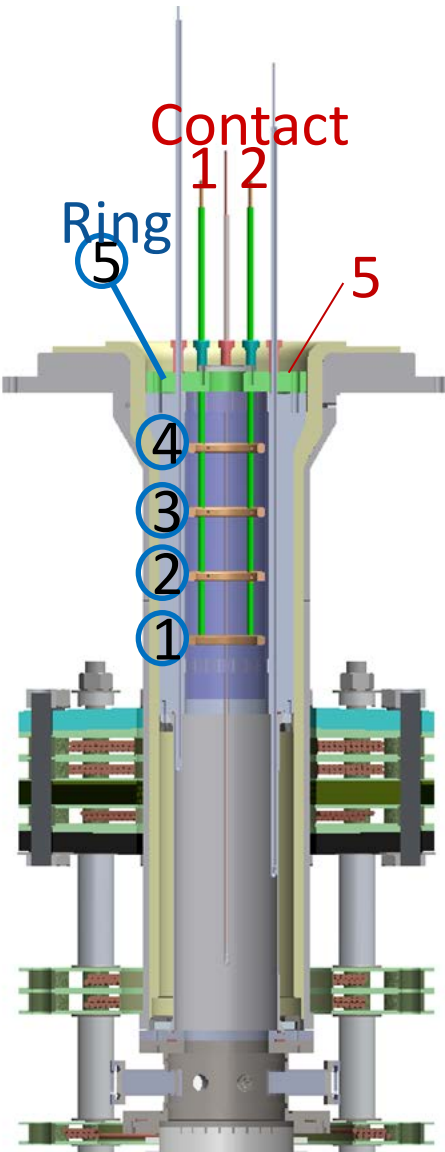
<sup>10</sup> T. Asai, et. al., "New control methods for stabilization and equilibrium of a field-reversed configuration," Workshop on Innovation in Fusion Science (ICC2011) and US-Japan Workshop on Compact Torus Plasma, August 16-19, 2011, Seattle, WA.



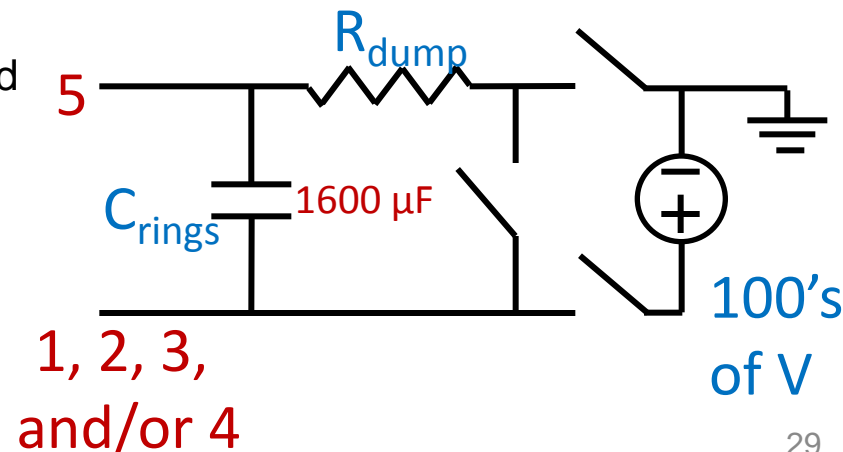
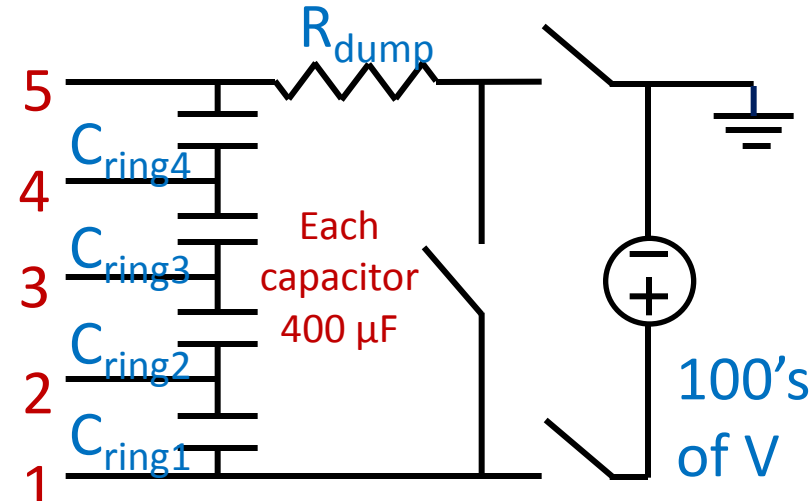
# The Biased Ring Assembly and Biasing Capacitor Bank



U.S. AIR FORCE



- Rings were initially unbiased; voltages that developed upon the rings were monitored during tests.
- The first biasing scheme (right) applied a graded voltage to the rings.
- From tests with a graded voltage, it was seen that 1 or more rings could be biased at the same voltage, while the others were left unbiased. This led to the next biasing scheme (lower right).
- Inductances in the bank and ring connections were reduced at this time to enable faster response of the bank in maintaining voltage on the rings.

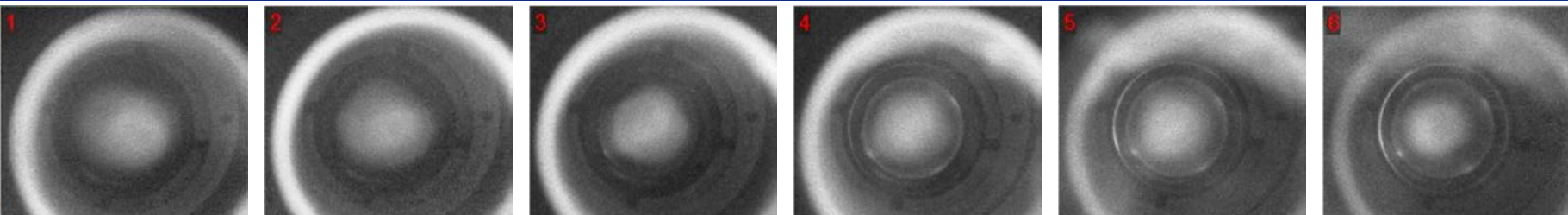




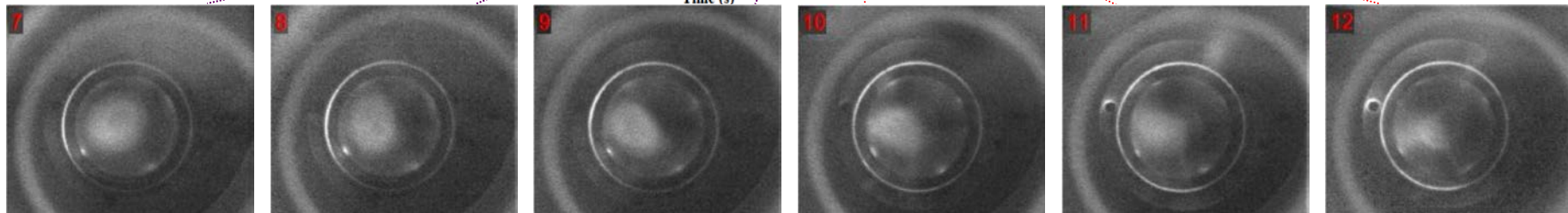
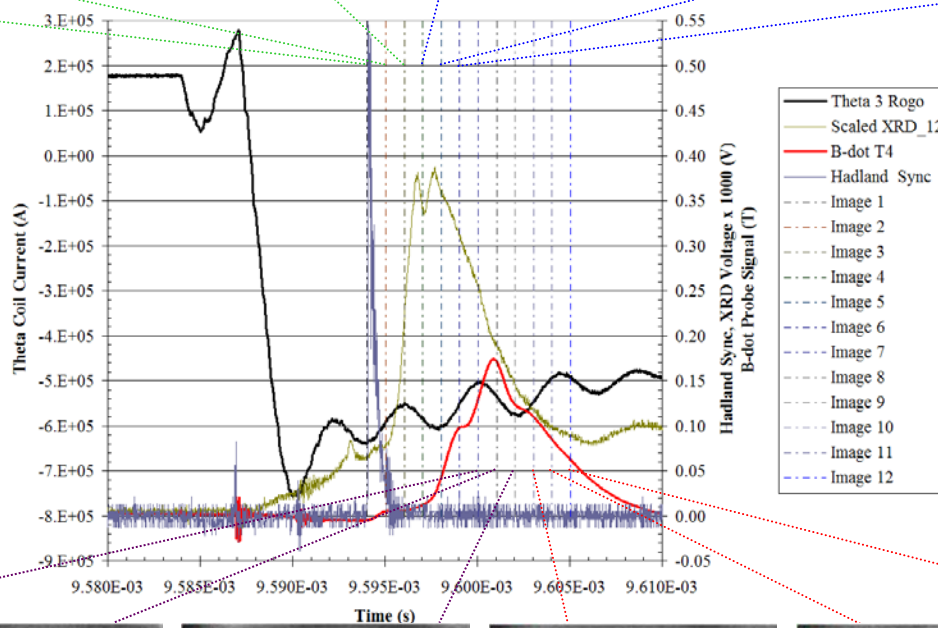
# Visible-Light FRC Plasma Observed to Remain Intact Longer



U.S. AIR FORCE



In keeping with the trends seen with the B-dot probes, break-up of the plasmoid begins later for this test, around frame 10 or 11, compared to frames 6 - 8 where it was observed for the 600V and 800V tests.



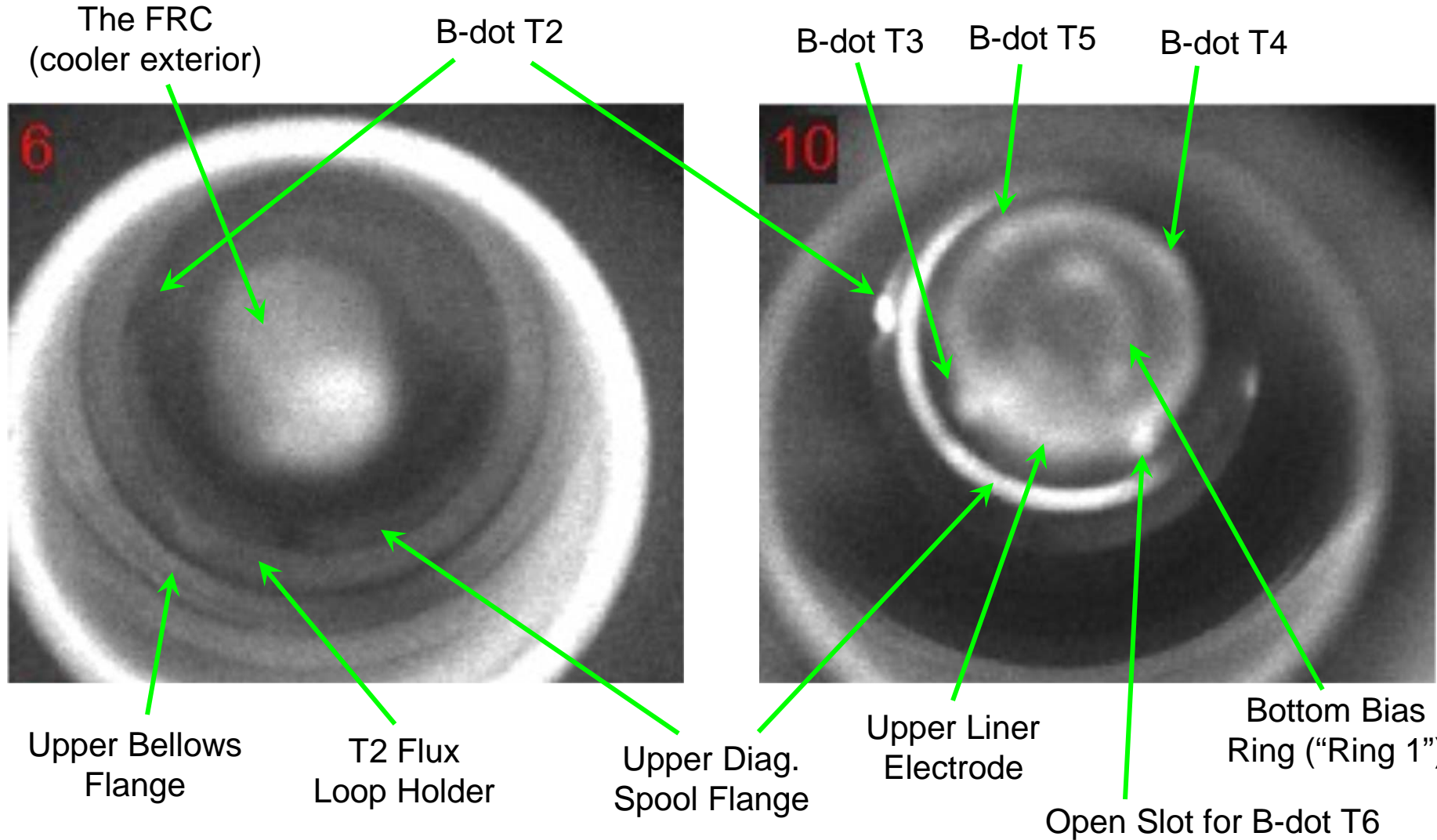
900V Ring Bias test –  
Image 1 @ 9.59404 ms  
(10.22  $\mu$ s after PI start); 1  $\mu$ s between frames, 100 ns exposure.



# LANL Hadland Fast Framing Camera is used to Image the Plasma



U.S. AIR FORCE



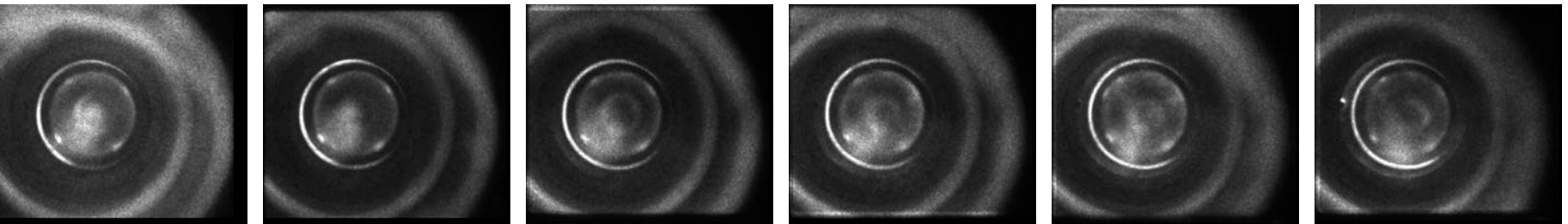
8  $\mu$ s between these two frames, 100 ns exposure

Distribution Statement A: Approved for public release; Distribution unlimited.



# Late time optical Evidence of Plasma Rotation

U.S. AIR FORCE



Plasma rotation inferred from images by noting changes in angular position of plasma features from frame to frame.

Note slowing of rotation in later frames.

(Motion is more evident when the frames are viewed as a movie.)

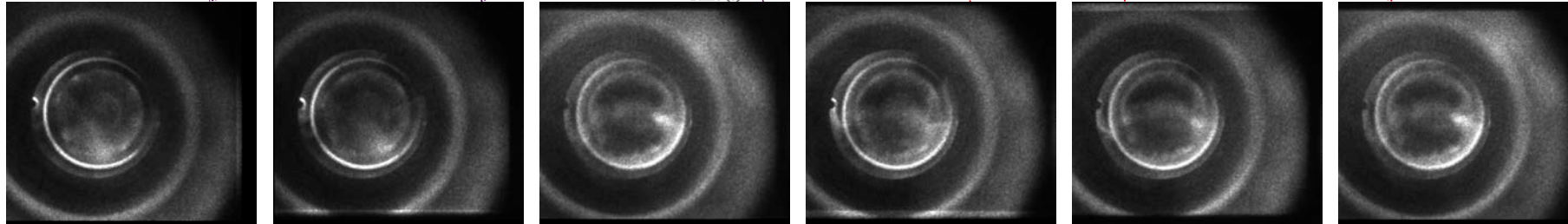
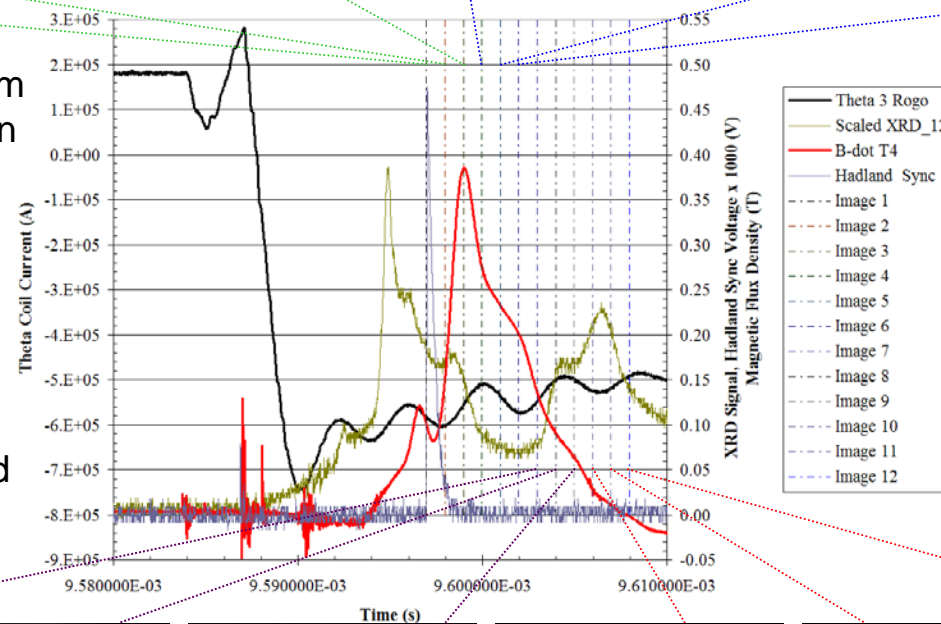
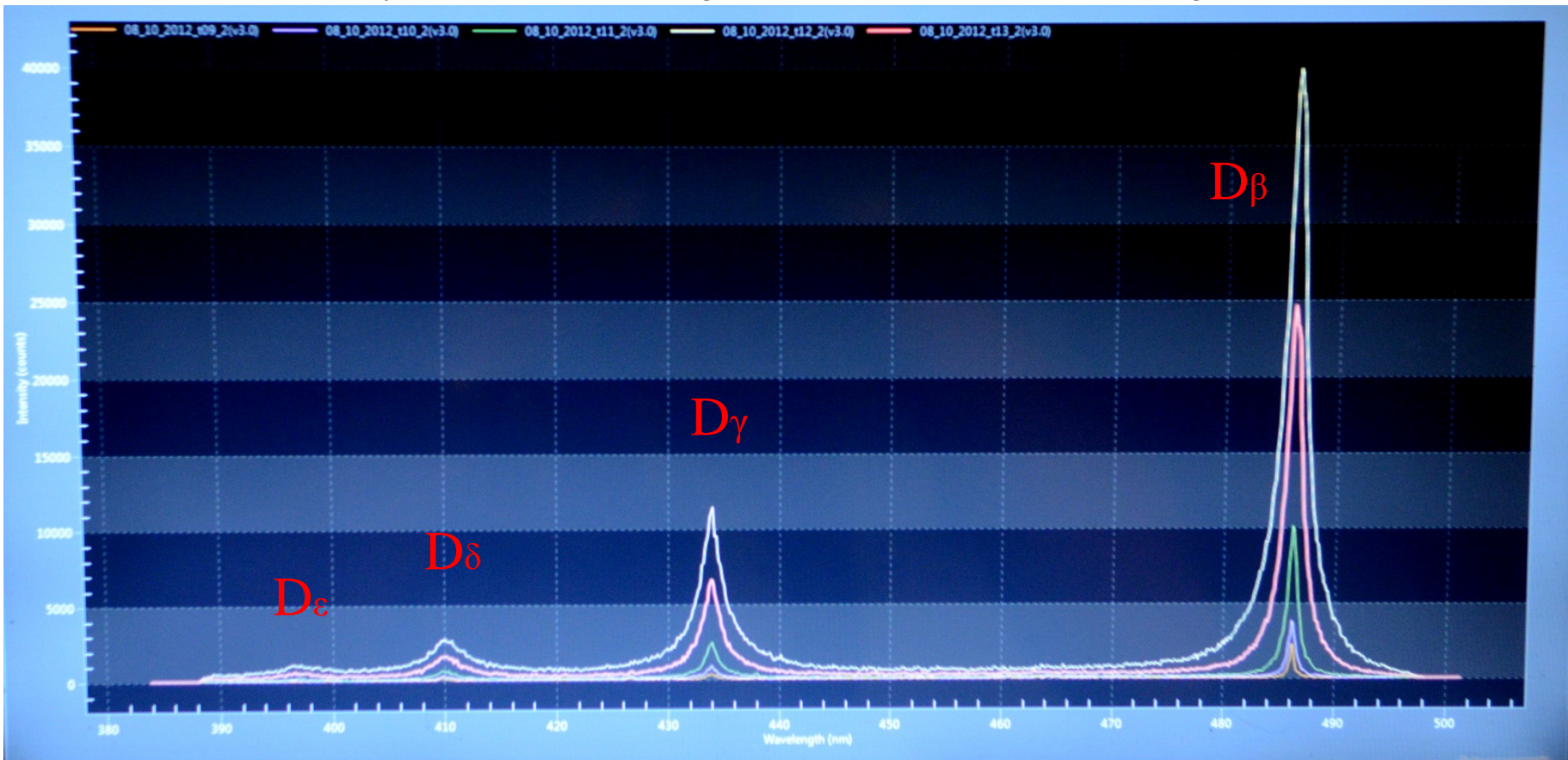


Image 1 @  
9.59697 ms  
(12.97  $\mu$ s after  
PI start); 1  $\mu$ s  
between frames,  
100 ns exposure.

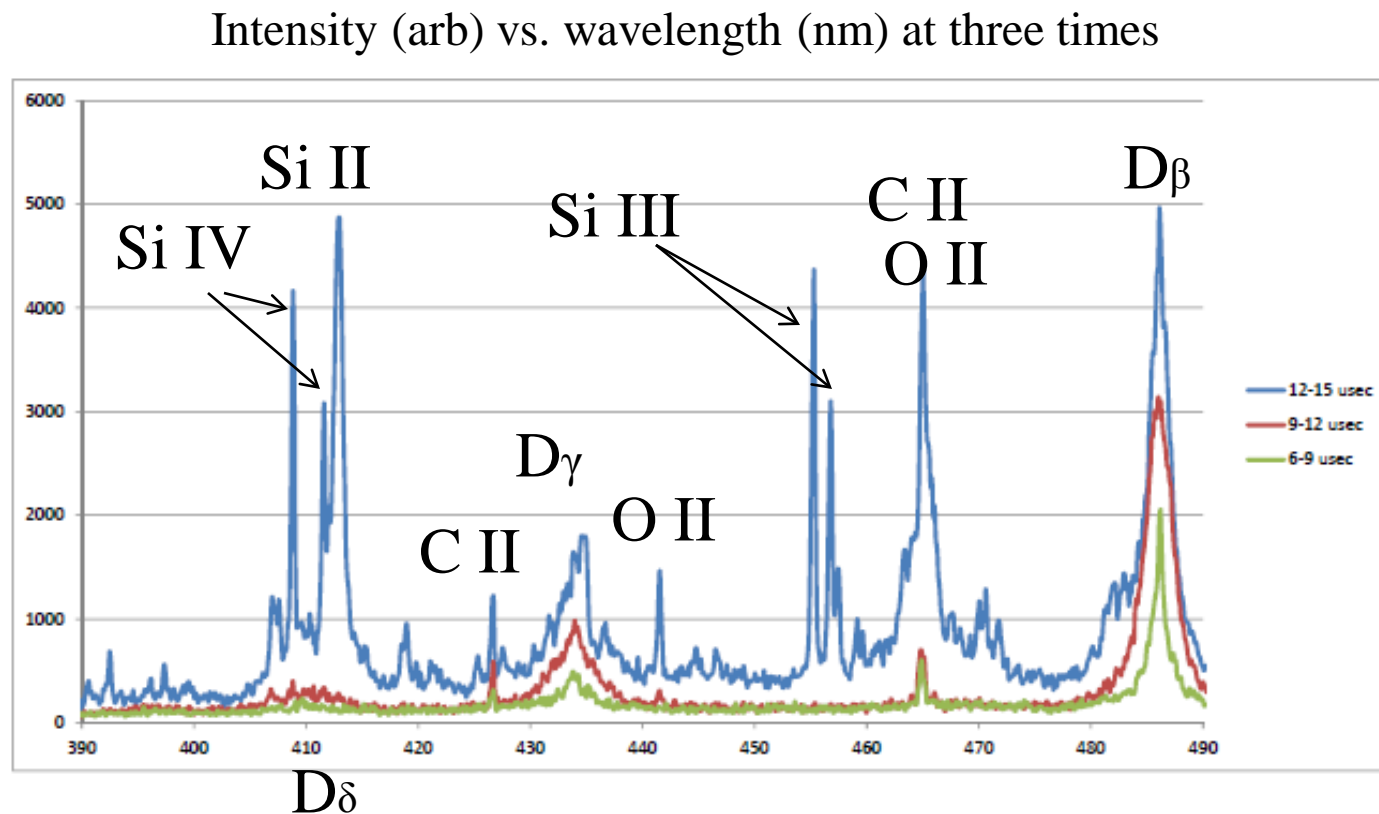
# During FRC formation (3-6 $\mu$ sec), the deuterium plasma is clean. Scan of static fill pressure

Intensity (arb) vs. wavelength (nm) (390-500 nm coverage)



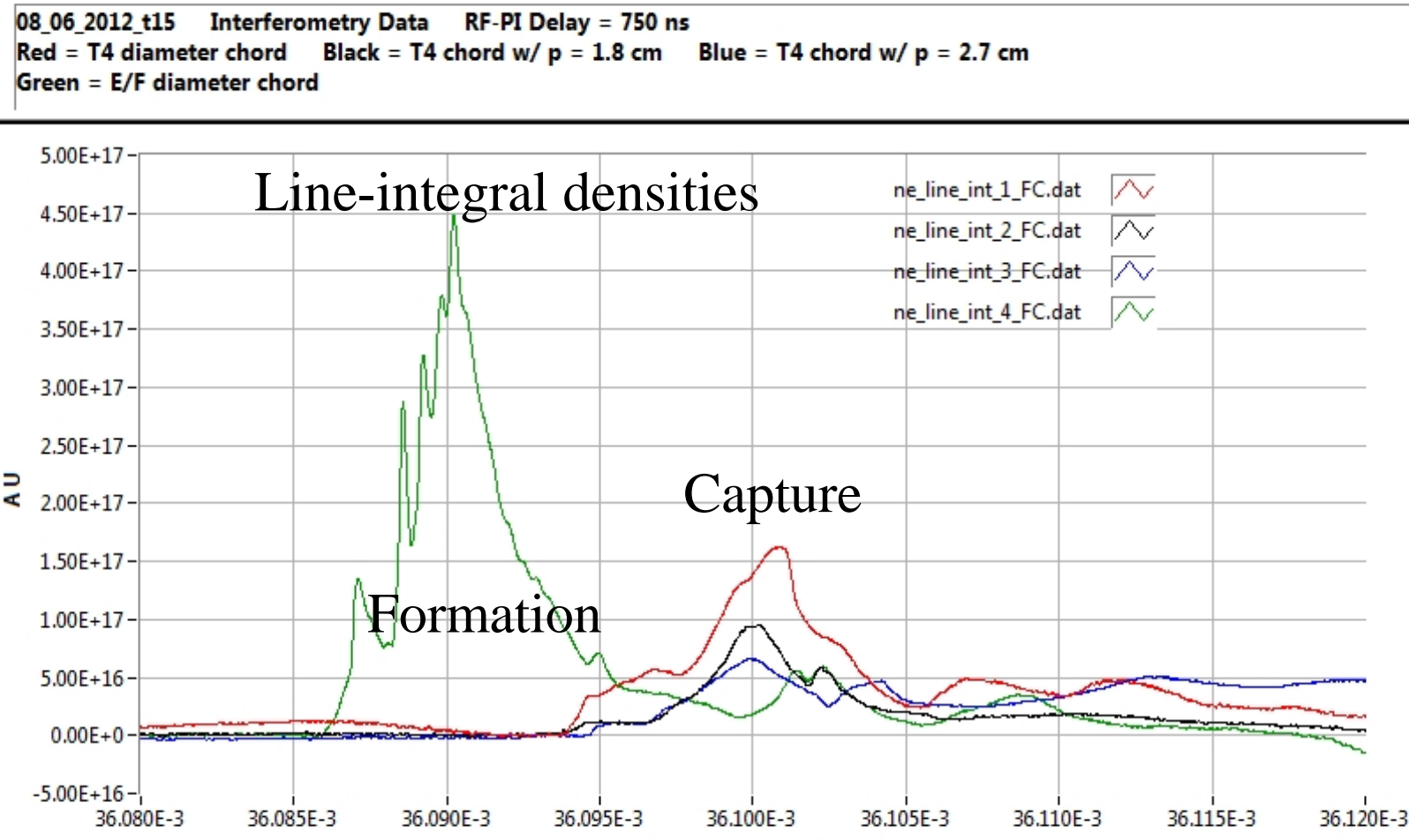
Optical spectra obtained with axial view, 3 microsecond exposure, show progressively brighter spectra (50, 75, 100, 150, 200 mTorr fill pressure), and increased Stark broadening, as expected. Classic Balmer series.

# Visible spectra show evidence of increased impurities at later times, as the plasma moves upwards



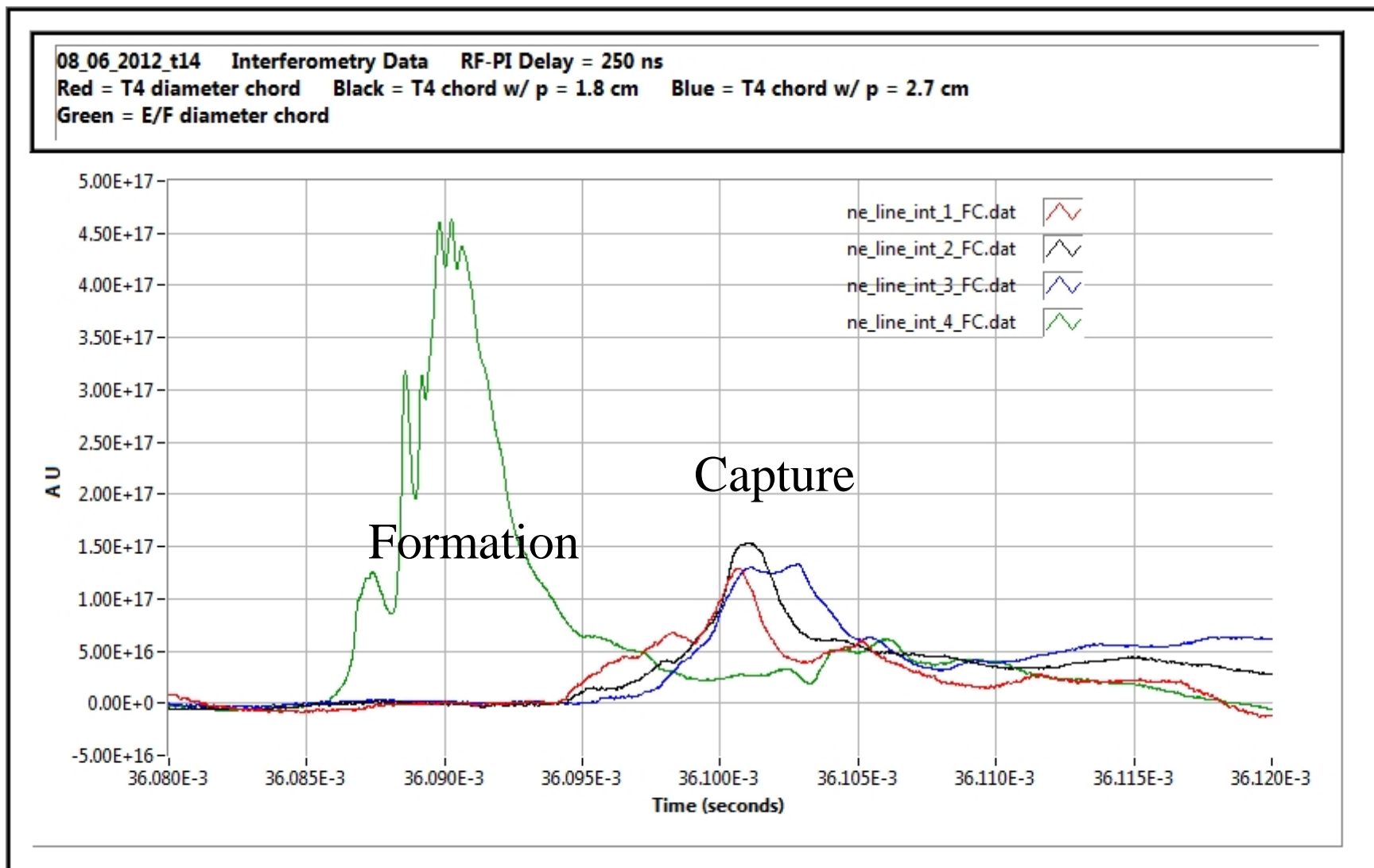
Optical spectra obtained with axial view, 3 microsecond exposure indicate few impurities until FRC reaches lower (entrance) implosion electrode 8 cm diameter aperture. The later time shows evidence of quartz tube interaction (or probes getting hit). We need to do this measurement with a narrower field of view.

# All three interferometer chords in capture region providing good data



A “normal” FRC decay is seen in the capture region here: density (line integrated) rises on all three chords and then falls off on all three chords.

With the three interferometer chords in the capture region providing data now, it is possible to see changes to the FRC that the Hadland images have been showing us in earlier tests

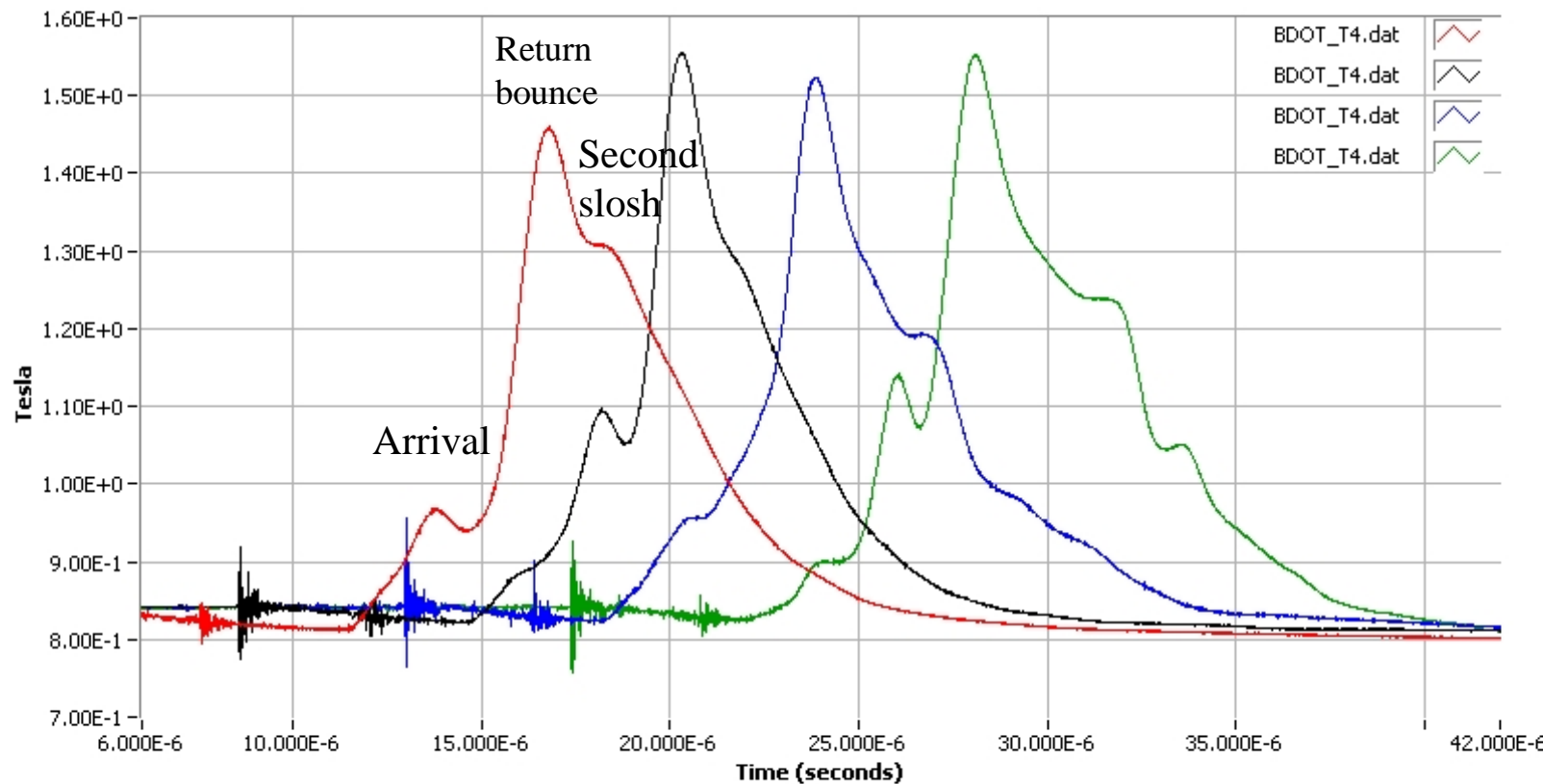


Something anomalous happens to the FRC at 36.099 and at 36.101 ms as the on-diameter chord (red) drops abruptly => the FRC appears be moving off-axis

# How does the captured plasma vary when the delay of the PI-to-Main Bank timing was extended to 2 or more PI periods?

Surprisingly, delaying looks like a good thing

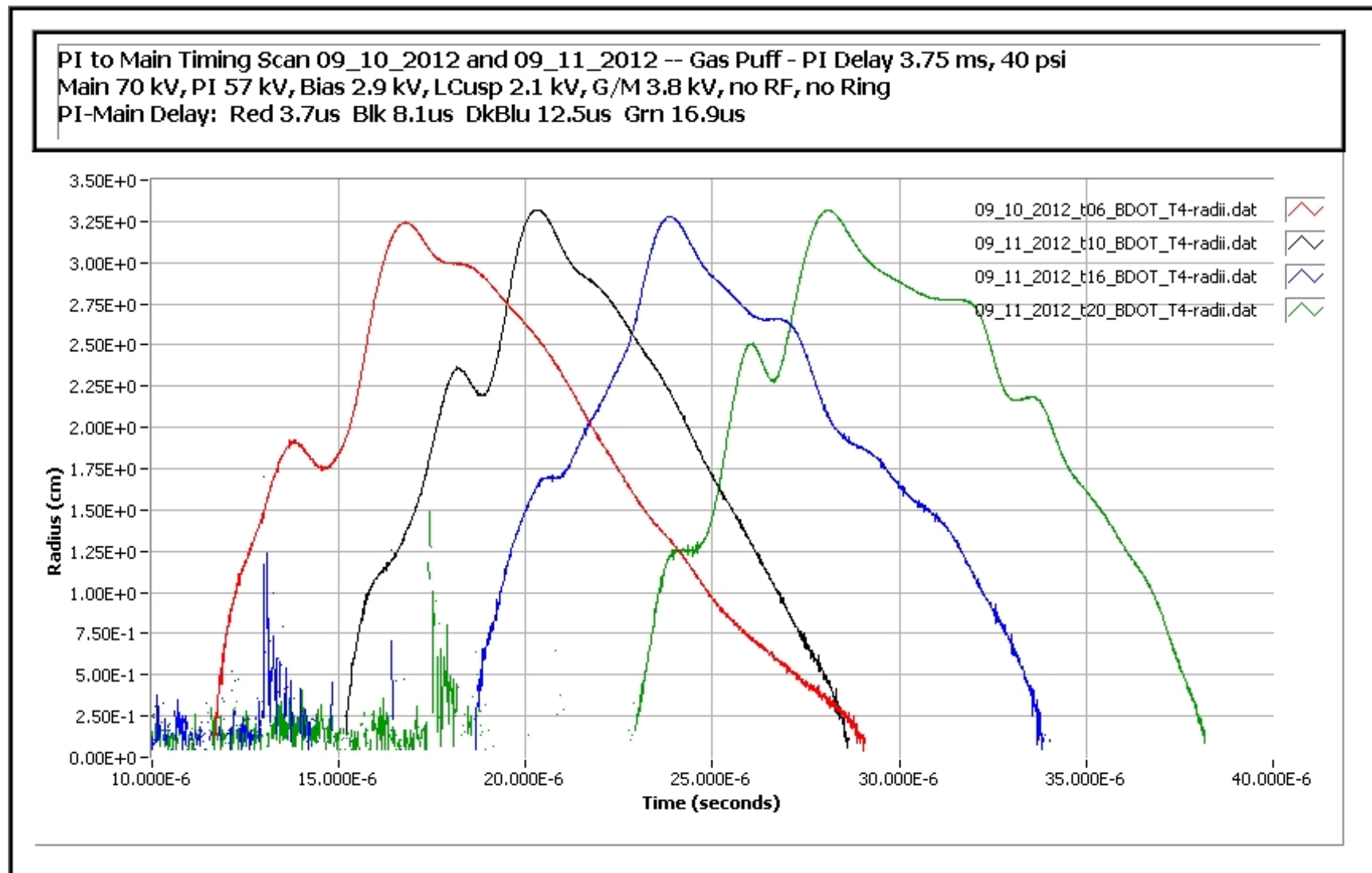
PI to Main Timing Scan over multiple PI periods 09\_10\_2012 and 09\_11\_2012 --  
Main 70 kV, PI 57 kV, Bias 4.9 kV, LCusp 2.1 kV, G/M 3.8 kV, Gas Puff 40 psi 3.75 ms, no RF, no Ring  
PI-Main Delay: Red 3.7us Blk 8.1us DkBlu 12.5us Grn 16.9us



Plotting integrated B-dot probe signal (at the wall) from center of capture region

# Excluded flux radii, $R_{\text{ex\_fl}}$ , calculated for the T4 B-dot waveforms on the previous slide

Lifetimes (FWHM) vary from  $8 \sim 10 \mu\text{s}$ .



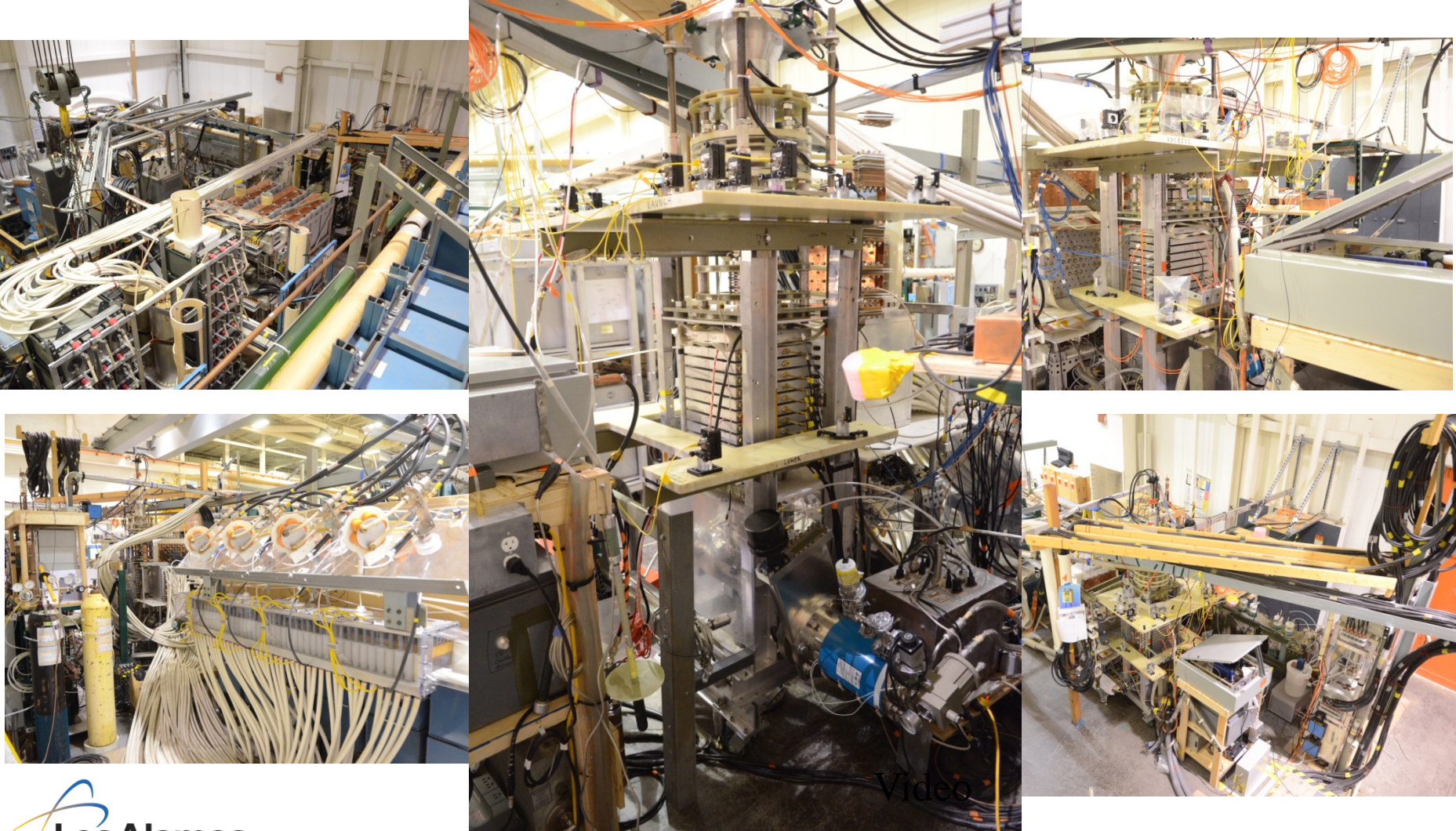
# Summary

---

- We have imploded a liner with interior magnetic mirror field, obtaining evidence for compression 1.36 T field to 540 T. Our first plasma compression in April 2010, was an engineering success, but showed no compression signatures (for example, no increased x-ray or neutron emission).
- We are scanning parts of parameter space. We have reliably formed, translated, and captured FRCs in magnetic mirrors inside metal liners in preparation for compression by liner implosion
- We have used two types of RF first stage ionization to improve FRC formation, but with only minor effect.
- We have implemented gas puff fill (instead of static fill) to enable higher voltage biased rings for rotation control.
- Observed via fast axial view photography evidence of rotation of translating and trapped FRC, and evidence of slowing of that rotation when biased rings used – however this slowing occurs after the FRC has deteriorated.
- Observed optical photography evidence for low contamination until FRC reaches lower (entrance) implosion electrode aperture – should do this with radial spatial resolution or collimation.
- We are planning 4 implosion shots. For the next implosion test in ~Dec 2012, we will separate the translation and mirror banks, to enable a delay the start of the FRC formation by 10-12 microseconds....so some FRC will be left by the time of peak implosion.
- For the follow-on tests in FY13, we may lengthen the trapping region, to better trap a higher flux FRC, and shorten the translation section (to reduce losses in transit).

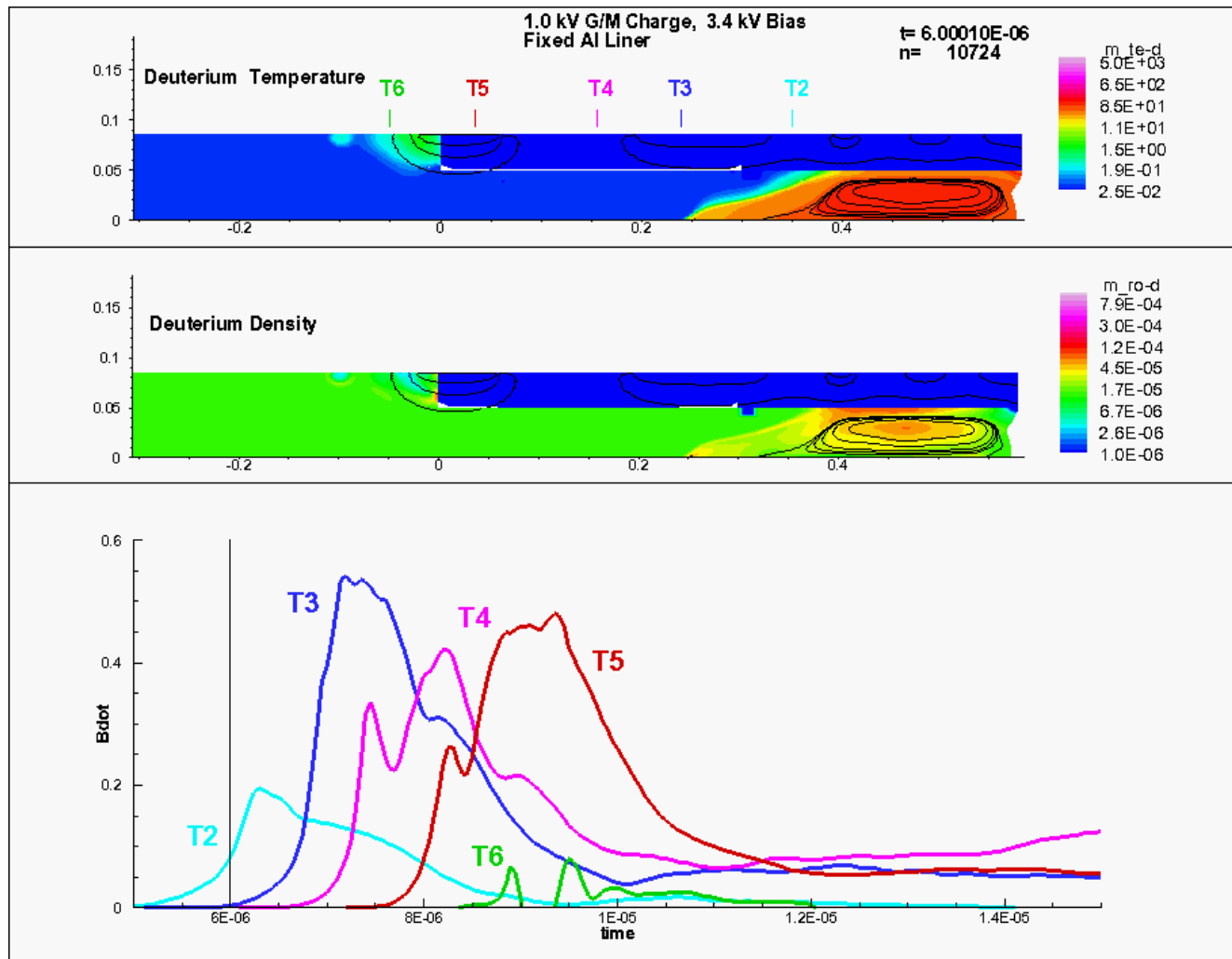
# FRCHX: a complex machine with a large crew

It takes 1 week to replace a broken quartz tube, and only about 30 microseconds to implode the front end, but longer than a month to shoot another implosion shot.



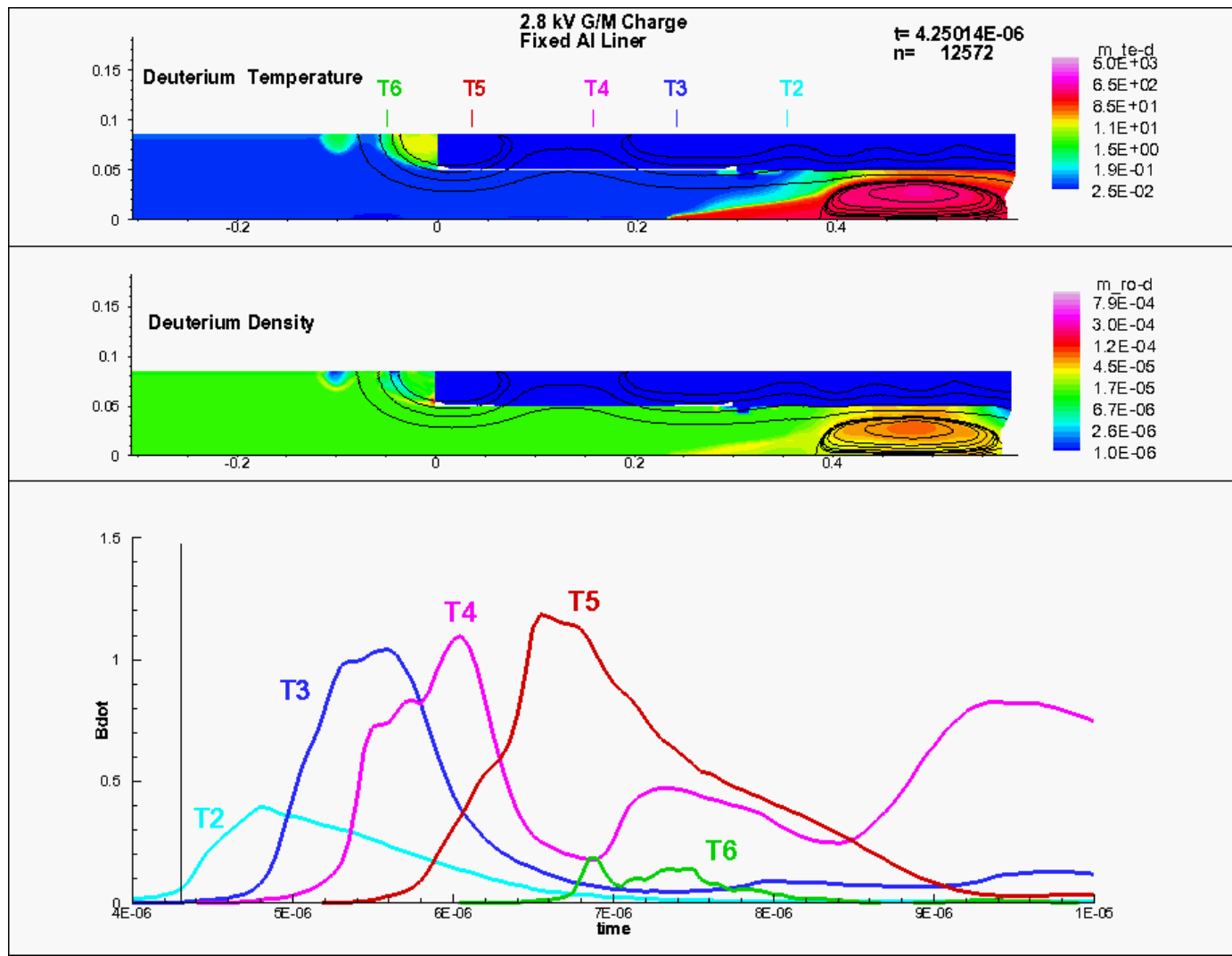
Video

# Data from probes at various axial locations are compared to NumerEx modeling

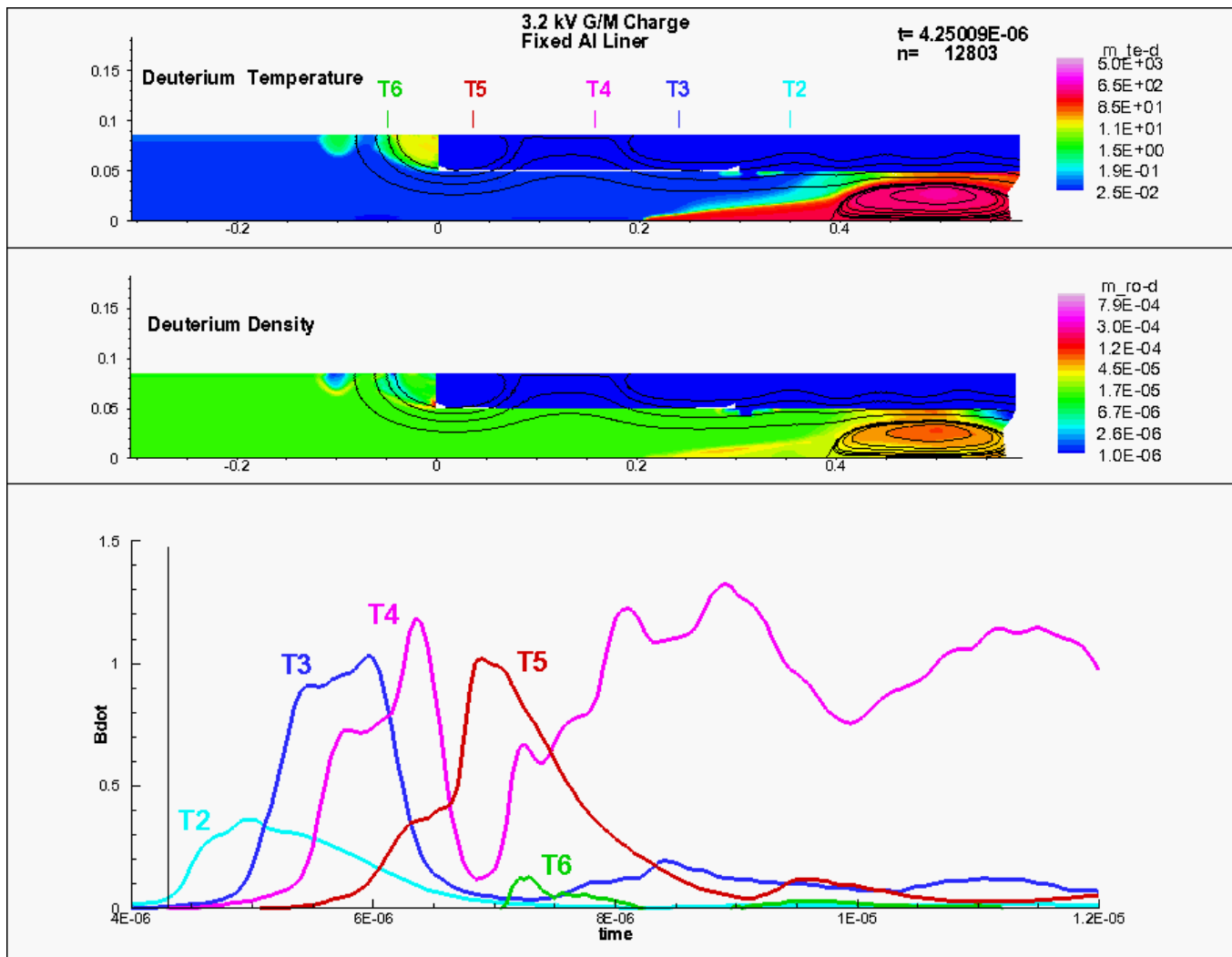


Here, the guide/mirror bank is too weak

# If the capture fields are not correct.....you don't trap the FRC that you went to all that trouble to make.....partial capture in this example



**Better (but not yet optimal capture).** Remember, than in an implosion shot, these fields are also changing in time, as the liner compresses.

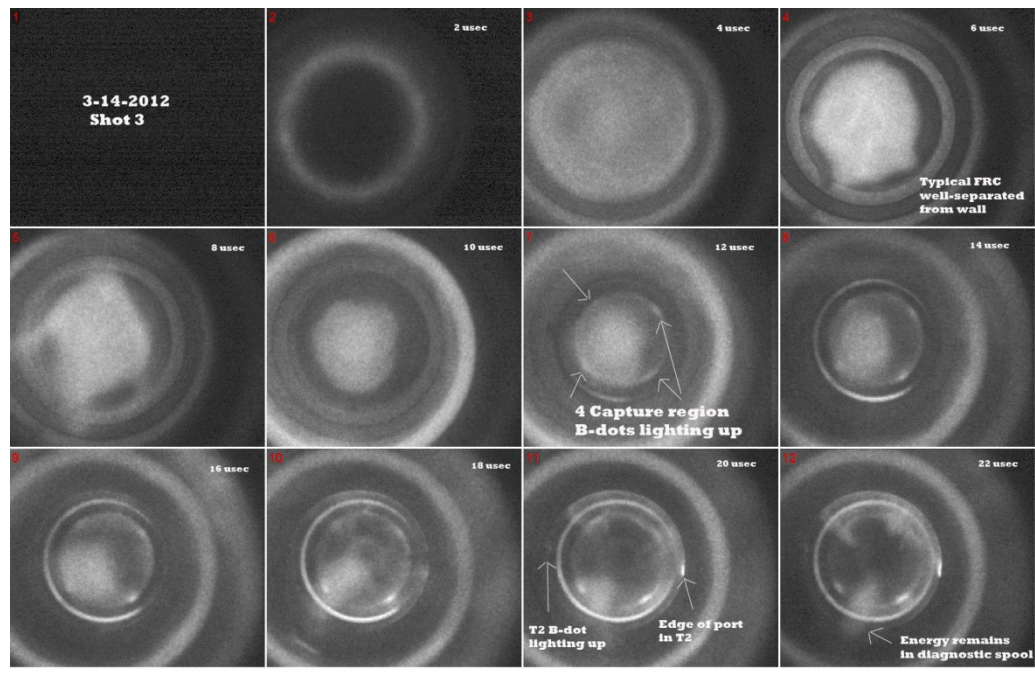
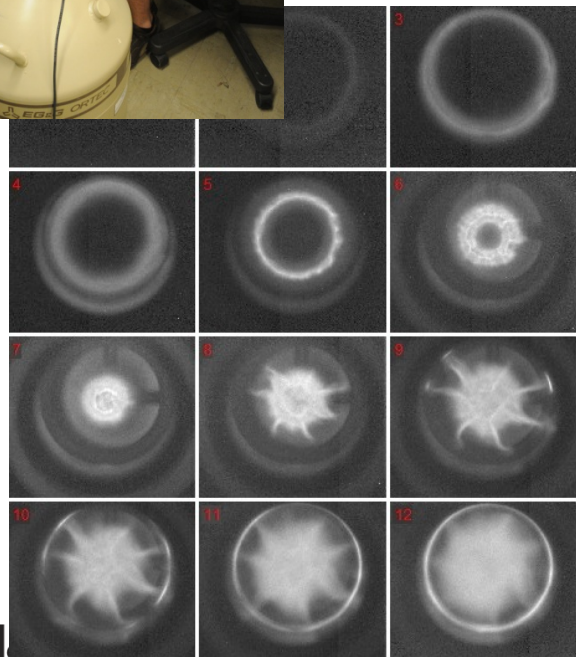
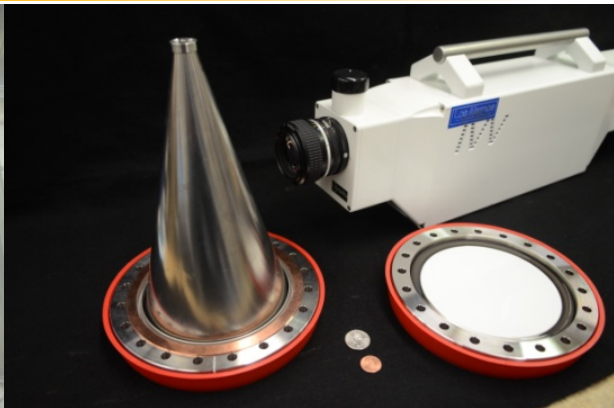
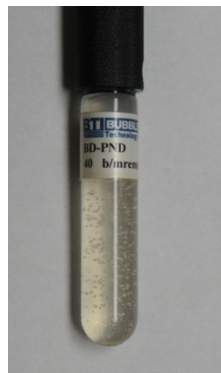
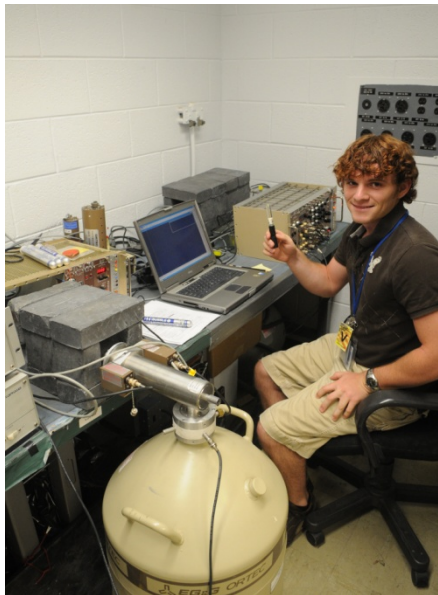


# LANL diagnostic systems at AFRL right now:

---

- 1). Snap-shot (single time, full spectrum) visible imaging spectroscopy, from 400-500 nm wavelength, gated, intensified, with PiMax camera and McPherson 218 spectrometer.
- 2). Single wavelength PMT on another McPherson 218, for time history of individual visible lines
- 3). Two sets of 7-channel soft x-ray diodes (in vacuum)/ changeable foils. One for side on, one for end-on viewing. With amplifiers as needed.
- 4). Shoebox 16-channel PMT array for monitoring H-alpha or H-beta at multiple spatial locations, with 400 micron fibers , and ball-lens chordal array fixture
- 5). Hadland 12-frame, visible camera, hardened, shielded, end-on imaging in the visible
- 6). Soft x-ray fluorescer convertor window and dunce-cap pinhole camera for multi-frame higher energy imaging (EUV to soft x-ray, depending on filters).
- 7). Amplified photodiodes to compare with AFRL ones for other formation monitoring, and RF preionization light monitors
- 8). Copper-activation neutron detector gear. Neutron bubble detectors. HPG gamma spectrometer for Indium activation. (The copper system was used on Trident neutron generation experiment recently not the recent Press Release), and has also been cross calibrated at Sandia.
- 9). Fiber-optic trigger units for data acquisition and various instrument triggering, as well as air-conditioned shielding Hofman box rack, with PXI crate full of 16-channel National Instruments 40 MHz digitizers, and smaller shielded rack for close-in neutron diagnostics (As-activation, Li-6, Pilot-B).

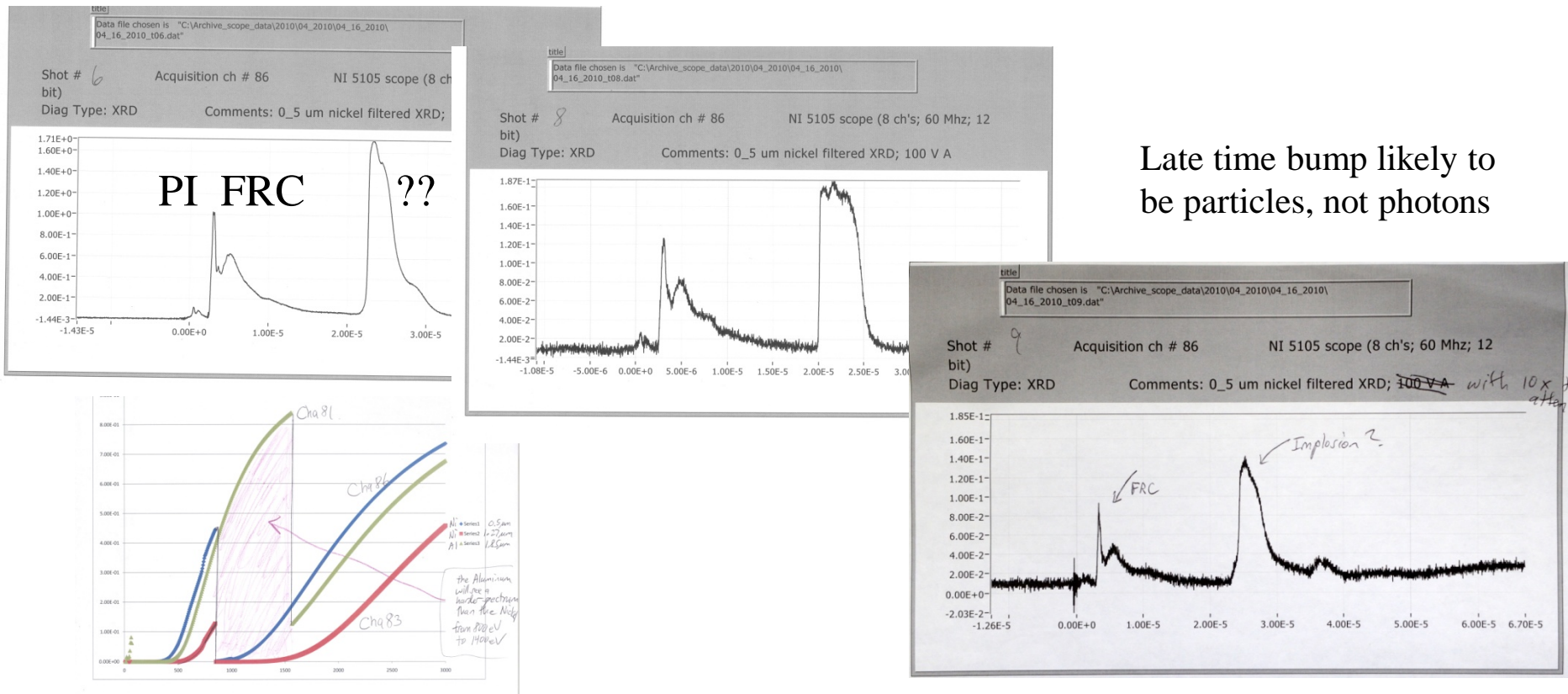
# Some of the LANL diagnostics at FRCHX



UNCLASSIFIED

# The case of the false “implosion” signal

- We had multiple types of soft x-ray diagnostics on the April 16, 2010 implosion shot, all viewing from the bottom of FRCHX. Weak signals (compared to what we expected) were seen in the vicinity of 22-25 microseconds...ie, implosion time. Shot 9 was the implosion.



Shot 8 had the gain turned down, in preparation for Shot 9. Shots 6 and 8 have the same feature....but things were so hectic, they weren't looked at until the day after...

UNCLASSIFIED

46

# Aftermath of April 16, 2010 Shot

---

